ISSN 2162-5298 (Print)
ISSN 2162-5301 (Online)
DOI:10.17265/2162-5298

David Publishing Company
www.davidpublisher.com

Journal of Environmental Science and Engineering A

Volume 7, Number 4, April 2018

From Knowledge to Wisdom

Journal of Environmental Science and Engineering A

Volume 7, Number 4, April 2018 (Serial Number 70)

David Publishing Company
www.davidpublisher.com

Publication Information:
Journal of Environmental Science and Engineering A (formerly parts of Journal of Environmental Science and Engineering ISSN 1934-8932, USA) is published monthly in hard copy (ISSN 2162-5298) and online (ISSN 2162-5301) by David Publishing Company located at 616 Corporate Way, Suite 2-4876, Valley Cottage, NY 10989, USA.

Aims and Scope:
Journal of Environmental Science and Engineering A, a monthly professional academic journal, covers all sorts of researches on environmental management and assessment, environmental monitoring, atmospheric environment, aquatic environment and municipal solid waste, etc..

Manuscripts and correspondence are invited for publication. You can submit your papers via Web Submission, or E-mail to environmental@davidpublishing.org, environmental@davidpublishing.com or info@davidpublishing.com. Submission guidelines and Web Submission system are available at http://www.davidpublisher.com.

Editorial Office:
616 Corporate Way, Suite 2-4876, Valley Cottage, NY 10989, USA
Tel: 1-323-984-7526, 323-410-1082
Fax: 1-323-984-7374, 323-908-0457
E-mail: environmental@davidpublishing.org; environmental@davidpublishing.com; info@davidpublishing.com

Abstracted/Indexed in:
Googel Scholar
CAS (Chemical Abstracts Service)
Database of EBSCO, Massachusetts, USA
Chinese Database of CEPS, Airiti Inc. & OCLC
Cambridge Science Abstracts (CSA)
Ulrich's Periodicals Directory
Chinese Scientific Journals Database, VIP Corporation, Chongqing, China
Summon Serials Solutions
ProQuest

Subscription Information:
Price (per year):
Print $600, Online $480
Print and Online $800

David Publishing Company
616 Corporate Way, Suite 2-4876, Valley Cottage, NY 10989, USA
Tel: 1-323-984-7526, 323-410-1082; Fax: 1-323-984-7374, 323-908-0457
E-mail: order@davidpublishing.com
Digital Cooperative Company: www.bookan.com.cn

David Publishing Company
www.davidpublisher.com

Journal of Environmental Science and Engineering A

Volume 7, Number 4, April 2018 (Serial Number 70)

Contents

Journal of Environmental Science and Engineering A 7 (2018) 147-158
doi:10.17265/2162-5298/2018.04.001

Evaluation of the Impact of the Handling and Storage System of Petroleum Coke on PM_{10} Emissions in an Oil Refinery

Claudinei Guimarães[1] and Paula Merigue[2]

1. Department of Biochemical Engineering, School of Chemistry, Federal University of Rio de Janeiro, Rio de Janeiro 21941909, Brazil

2. Polytechnic School, Federal University of Rio de Janeiro, Rio de Janeiro 21949-909, Brazil

Abstract: The objective of this study was to identify the impact of the coke handling and storage system on the emission of PM_{10} particulate material. The methodology was based on AP-42 emission factors from U.S. EPA (United States Environmental Protection Agency) for the calculation of PM_{10} emissions from operations in the handling and storage of petroleum coke in an oil refinery in the northeastern of Brazil. The knowledge of the emission potential of each operation of the coke handling and storage system allows the adoption of more effective control measures, contributing to the effective reduction of PM_{10} emissions in this system. To complement the environmental impact assessment of each configuration, an air quality modelling was performed using the atmospheric dispersion software. The comparison performed in this study enables authors to conclude, even for a totally mechanic system, that adopts control measures, PM_{10} emissions are low when confronted with the remaining sources of an oil refinery. By analyzing emissions from automated systems operation (scenario 1), it can be observed that the source with higher emission potential is the stockpile, which represents 60% of the system's emission. Transfer and transport operations by conveyor belts together correspond to 40% of emissions. Even though transfer operations also represent a significant part (27%), they are not clustered in a unique point, making these emissions abatement difficult. The same is valid for transport using conveyor belts. Emissions from the piles are really the most significant. For this reason, this work concentrated efforts in the storage area, the ones that motivate the majority of studies relating to abatement technologies.

Key words: Emission factors, petroleum coke handling and storage system, environmental pollution, PM_{10} emissions, air quality modelling.

1. Introduction

The progress of studies that correlate the presence of PM (Particulate Matter) with atmosphere and health damage [1, 2], as well as better population awareness, has motivated the adoption of more restrictive legislations regarding emission standards for air pollutants. The most restrictive regulations concerning PM_{10} are in the European Community, Directive 2008/50/EC, which establishes the 24-hour mean of 50 $\mu g/m^3$ and annual mean of 40 $\mu g/m^3$ [3]. In the United States, the Environmental Protection Agency, sets the daily limit of 150 $\mu g/m^3$ that should not be exceeded more than once per year on average over a 3-year period [4]. The guideline values provided by the World Health Organization in its air quality guide [5] are 50 $\mu g/m^3$ for the 24-hour mean, similar to European limits, and 20 $\mu g/m^3$ for annual mean.

To reach the increasingly restrictive limits established by environmental agencies, it is necessary to reduce the emission rates of PM_{10} from all sources. For this reason, several studies seeking to identify the main sources either locally or globally [6, 7] showed that there is a great variation of the PM_{10} and $PM_{2.5}$ sources between the regions, either by the economic development or by environmental factors. However,

Corresponding author: Claudinei Guimarães, Ph.D., research field: atmospheric pollution.

emissions related to vehicle traffic were the ones that showed the highest percentage in most of the analyzed sites. The contribution of unspecified sources of human origin also has high values in most regions indicating that there is still a deficiency in the identification of certain PM sources. This deficiency was also perceived by Winiwarter, W., et al. [8] that analyzed the quality of European PM_{10} inventory based on several publications and concluded that there are still improvements to be made in the quantification of PM emissions, especially for PM_{10} fugitive emissions from less significant sources.

The main sources of PM emissions from an oil refinery are the furnaces and boilers that burn fossil fuels for power and steam generation to the process units. In addition to these sources, another very relevant one for PM emission is the flare that burns the relieved streams during the emergency scenarios and units' start-ups and shutdowns. In relation to the process units, the FCC (Fluid Catalytic Cracker) units are mainly responsible for fugitive PM emissions due to loss of catalyst [9]. All of these sources are monitored and have several measures for abatement and reduction of PM emissions. However, there are less significant sources that are not monitored or accounted for in the total refinery inventory. An example that may be cited is the petroleum coke handling and storage system. This system is necessary for expedition of coke produced in DCU (Delayed Coking Unit) that exists in great part of oil refineries around the world. Such units are responsible for increasing of conversion and profitability of refineries.

Emissions from handling and storage of petroleum coke considered fugitive emissions, so it is difficult to monitor and quantify them by direct measurements. PM_{10} emissions from this system are a consequence of the system's configuration applied, production features and also local climate conditions [10]. Due to these many variables that contribute to the emissions, the use of a generic emission factor might not represent real emissions in this system.

Considering these difficulties, this work aims to draw a methodology to estimate emissions in the coke system handling and storage, taking into consideration the main variables that interfere in these emissions. Estimates considered each system operation so that different configurations could be compared. The most usual abatement measures for these systems were also analyzed. In order to evaluate the impact of emissions of this system on air quality, an atmospheric dispersion modelling was performed. For the study, a recent installation of this system was considered in an oil refinery in Brazil.

2. Material and Methods

2.1 Emissions Calculation

PM_{10} emissions from handling and coke storage system can be estimated through emission factors. It is possible to find in literature factors related to general handling and solids storage system, and also some specific factors to extraction activities and coal mining. However, there is no specific information to petroleum coke system. This cannot be a limitation for the use of these factors, since some of them are expressed in terms of properties that allow extrapolation for several solids, by considering dusts content and solids humidity in their calculations [11]. AP-42, Compilation of Air Pollutant Emission Factors, has been a benchmark on emission factors, such as technical guides of Australian Agency [12] and European Community [13], whose methodologies are based on AP-42 factors. Application of emission factors available in AP-42 for different industrial processes is a recurring practice and shows adherence if compared to experimental data when this comparison is possible [14].

The level of emissions of operations like handling and petroleum coke storage depend on the system configuration and automation level. More automated systems have equipment such as stackers and reclaimers to insert and remove coke from piles, respectively, conveyor belts to transport the coke from cokepad to

stockyard and then to loading silos/expedition or rail loading. In less automated systems coke handling is done with the aid of wheel loaders that can be used only to remove coke from piles and load it on wagons or truck buckets or even to form stockpiles.

The emission factors listed in AP-42 are aimed at a specific activity. In order to use them in handling and coke storage system inventory, it was necessary to share the system in their different activities, selecting the factors that best fit into the activities present in coke system. Given the possibilities, five major operations were identified, which can be present in handling and coke storage system and contribute significantly for PM_{10} emissions:

Handling: handling activities are characterized by coke transfer operations, such as the transfer of the coke from cokepit and cokepad, stockpiles formation, coke loading for expedition, transfer between conveyor belts, etc.。 Each transfer operation contributes to PM_{10} emissions according to the rate presented in U.S. EPA AP-42 Manual (Chapter 13.2.4) [15]:

$$EF_h = 0.0016 k_h \frac{(U/2.2)^{1.3}}{(M/2)^{1.4}} \quad (1)$$

Eq. (1) [kg PM per tonne of coke handling] is the emission factor from handling, k_h [dimensionless] is the particle size multiplier, U [m/s] is the mean wind speed and M [%] is the coke moisture content.

Conveying: coke transfer on conveyor belts between cokepad and stockyard and from stockyard to loading silos/expedition. During transportation, particle material falls from conveyor belts or failures such as overflowing and belt misalignment can occur. Emission from conveying can be estimated by Eq. (2) proposed by TCEQ [16]:

$$EF_c = 0{,}0016 k_c \frac{(\mathrm{U}/2.2)^{1.3}}{(\mathrm{M}/2)^{1.4}} \left(\frac{L_c}{304.8}\right) \quad (2)$$

Eq. (2) [kg PM per tonne of coke conveying] is the emission factor from conveyor belts operations, k_c [dimensionless] is the particle size multiplier, U [m/s] is the mean wind speed, M [%] coke moisture content and L_c [m] is the length of conveyors.

Storage pile wind erosion: particle material in open stockpiles is subject to erosion caused by wind action, which is an important PM emission source. These emissions can be calculated by methodology proposed in the fourth edition of the U.S. EPA AP-42 Manual [17]:

$$EF_w = 1.7 k_w \left(\frac{s}{1.5}\right)\left(\frac{365 - N_p}{235}\right)\left(\frac{f}{15}\right) \quad (3)$$

Eq. (3) [kg PM per day per hectare of pile] is the emission factor from storage pile wind erosion, k_w [dimensionless] is the particle size multiplier, s [%] is the material silt content, N_p [dimensionless] is the number of days with rainfall precipitations above 0.254 mm in the year and f [%] is the percentage of time that the unobstructed wind speed exceeds 5.4 m/s at the mean pile height.

Loading by wheel loader: when wheel loaders are used to handling coke, either in stacking or expedition section, there is a great potential of PM emission. The use of this equipment contributes to the increase of silt present in the coke which is more easily emitted during transfer and storage operations. The equation proposed by U.S. EPA AP-42 Manual [18] to estimate the emission from this type of operation is given:

$$EF_B = k_B \frac{(s)^{1.5}}{(M)^{1.4}} \quad (4)$$

Eq. (4) [kg PM per hour of wheel loader use] is the emission factor related to the use of wheel loader, k_B [dimensionless] is the particle size multiplier, s [%] is the material silt content and M [%] is the material moisture content.

Transport on unpaved roads: in systems that do not have loading silos, loading is performed directly on the stockyard using wheel loaders. During these operations, trucks are used to transfer the stored material, increasing silt content which in consequence contributes to PM emissions. The calculation of emissions can be done by the equation provided by U.S. EPA AP-42 Manual (Chapter 13.2.2):

$$EF_U = 281.9 k_U \left(\frac{s}{12}\right)^{\mathrm{a}} \left(\frac{W}{3}\right)^{\mathrm{b}} \quad (5)$$

Eq. (5) [g PM per vehicle kilometer traveled] is the emission factor for transport on unpaved roads, k_U [dimensionless] is the particle size multiplier, s [%] is the material silt content and W [t] is the mean vehicle weight. Emission rates were calculated according to the Eq. (6), considering the emission factors presented in Eqs. (1)-(5):

$$E_i = A_i \times EF_i \times (1 - ER_i/100) \quad (6)$$

Eq. (6) is the emission rate for activity i, A_i is the activity rate for activity i, EF_i is the emission factor for activity I and ER_i is the emission reduction efficiency for activity i.

Emission factors presented in Eqs. (1)-(5) did not consider the use of abatement technologies or other measures that contribute to emission reduction. Emission reduction due to the presence of mitigating measures was considered in the emission reduction ER (Efficiency Variable), as described in Eq. (6).

The main technologies used in handling and coke storage system for emission control and abatement were as:

(1) High humidity content in the material during handling/storage: the humidity content varies from 8 to 12% during handling and storage phases. This value is considered high and contributes to minimizing PM emissions.

(2) Covered or closed conveyor belts: coke transportation on belts, either covered or closed, reduces emission as it avoids material falls and overflowing during transportation.

(3) Confined transfer points (change in belts direction): when coke transfer between belts is carried out indoors, emissions from these operations are minimized.

(4) Water and/or chemicals aspersion in stockpiles: material that is stored outdoors might lose natural humidity and thus enable PM emission. Wetting is a recommended practice to keep humidity and reduce emission in piles caused by wind action. Some chemicals agents such as humectants or surfactants substances maximize the wetting effect.

(5) Protection against wind action on stockpiles: protecting material stored against wind action is an important measure to minimize and/or avoid emission. Among the possibilities are wind screens, which can reduce the intensity when wind reaches piles, and even total coverage of stockyard.

The measures listed above correspond to the best available technologies according to institutions such as Ref. [19], European Commission for pollution control and prevention [20] and Australian Government (National Pollutant Inventory). Besides all measures previously mentioned, other actions complement the list, for instance, piles configuration on stockyard, preventive maintenance to avoid damages to conveyor belts and use of appropriate machinery for coke formation and removal from piles (stackers and reclaimers).

Abatement measures listed in Table 1 were adopted in this work. The potential emissions reduction for each selected measure was obtained from the references mentioned above. The value of the reduction potential of some control measures has divergences between the cited references. In these cases, the lowest value was adopted.

Three configurations were selected to evaluate the emission potential of each operation for handling and coke storage system. In order to allow a comparison among the analyzed cases, some parameters were maintained, such as handled coke volume and location of the stockyard.

Table 1 Potential emission reduction-control measures applied.

Operation	Control measures	Emission reduction
Conveying	Enclosure of conveyors	70%
	Enclosure of transfer points	70%
Storage	Water spraying	50%
	Windbreaks	30%

Scenario 1: Automated System

This configuration contemplates the use of specific equipment for coke transfer and handling, great part of which can be operated remotely, without the need of human presence in the area, thus being called automated system in this work. Cranes or semi gantries were used to transfer the coke from cokepit to cokepad and then to sliding hopper. The coke is forwarded to storage patio using conveyor belts. Pile formation in the stockyard is done with stackers and coke removal from the piles for expedition is performed with reclaimers. Coke is again transferred through conveyor belts to road or rail loading silos. Coke loading onto trucks or wagons is done with a telescopic hauling that guides the coke, avoiding spilling.

Scenario 2: Semi Automated System

This configuration is called semi-automated because it has equipment that can be operated remotely in stacking section and equipment that need human supervision to be operated in expedition section. Up to the moment of piles formation this system operates exactly like the automated one. The main difference appears at the moment when the coke is reclaimed from the piles, which is done with the aid of wheel loaders and not by reclaimers. Truck or wagon loading is done directly in the storage area by wheel loaders with vehicles moving over the stored material.

Scenario 3: Mechanic System

In the mechanic configuration, all coke transfer and handling are done under human supervision, there are not operations that can be made remotely. Coke transportation from cokepad to stockyard is done from trucks that are loaded by wheel loaders. The trucks deposit the coke in the storage area and, again, using wheel loaders, piles are formed. Coke removal and expedition for trading occur by the same way as described in the semi-automated system.

According to the configuration of each proposed scenario, emissions of each activity were calculated in conformity with the emission factors (Eqs. (1)-(6)) and the potential reduction shown in Table 1. The activities considered in each scenario are listed in Table 2.

Table 3 presents the parameters considered in the calculations. The meteorological parameters, like mean wind speed, number of days with rainfall precipitations above 0.254 mm in the year and percentage of time that unobstructed wind speed exceeds 5.4 m/s were obtained from the meteorological data of the region selected for the study. For that, the average values of a three-year period were considered. The physical properties such as moisture and silt content can be obtained from the literature (typical values) or experimentally. In this work, the typical values suggested by Ref. [21] were used. The operational parameters were selected from a coke handling and storage system of an oil refinery.

Two variations for each scenario were considered for comparisons: in the first one credit was not given to existing control measures and in the second one control measures present in the system were considered. The same control measures were applied in the three scenarios to allow comparison. The use of emission factors makes it possible to estimate the emission rates in each activity and thus to evaluate which operations present in handling and coke storage system most contribute to PM emission. Nevertheless, to quantify the impact of these emissions in terms of air quality it is necessary to carry out an atmospheric dispersion study. Results of such study will allow a comparison with air quality values practiced and recommended by legislations.

2.2 Atmospheric Dispersion Modelling Study

Dispersion modelling uses mathematical formulations to characterize the atmospheric process that disperses a pollutant emitted by a source, based on emission rate, source data and meteorological inputs. For this study utilized the software AERMOD, a commercial atmospheric dispersion model recognized by U.S. EPA. AERMOD is a steady-state commercial model that allows the calculation of the concentration of a given pollutant from multiple sources, it takes into account

Table 2 Activities considered in each scenario for emissions calculation.

Scenario	Operation	Activity
Scenario 1	From cokepit to cokepad and/or to sliding hopper	Handling
	Belt conveyor system	Conveying
	Belt conveyor transfer stations	Handling
	Stacking coke (by stacker)	Handling
	Coke storage in open yard	Storage pile wind erosion
	Trucks loading	Handling
Scenario 2	From cokepit to cokepad and/or to sliding hopper	Handling
	Belt conveyor system	Conveying
	Belt conveyor transfer stations	Handling
	Stacking coke (by stacker)	Handling
	Coke storage in open yard	Storage pile wind erosion
	Reclaiming coke from stockpile (by wheel loader)	Loading by wheel loader
	Trucks loading	Handling
	Trucks transport on storage area	Transport on unpaved roads
Scenario 3	From cokepit to cokepad	Handling
	Reclaiming coke from cokepad (by wheel loader)	Loading by wheel loader
	Trucks loading	Handling
	Truck unloading on storage area	Handling
	Coke storage in open yard	Storage pile wind erosion
	Reclaiming coke from stockpile (by wheel loader)	Loading by wheel loader
	Trucks loading	Handling
	Trucks transport on storage area	Transport on unpaved roads

Table 3 Parameters used in calculation of emission rates.

Parameter	Value
Mean wind speed (U)	4.3 m/s
Moisture content (M)	10%
Material silt content (s)	5%
Number of days with rainfall precipitation above 0.254 mm per year (N_p)	82 days
Percentage of time that the unobstructed wind speed exceeds 5.4 m/s at the mean pile height (f)	22.5%
Mean vehicle weight (W)	30,000 kg
Particle size multiplier (k_i)	$k_h = k_c = 0.35$; $k_w = 0.5$; $k_B = 6.33$ and $k_U = 1.5$
Activity rate for handling and conveying (A_h, A_c)	6,144 t/d
Stockpile area (A_w)	22,214 m²
Hours of use of wheel loader (A_B)	13 h/day-6 days per week
Number of wheel loader	3
Vehicle distance traveled (A_U)	510 m
Number of vehicle per day	114

the Gaussian model for plume dispersion for stable atmospheric conditions. AERMOD has two data processors: (i) AERMET, a meteorological data preprocessor, and (ii) AERMAP, a terrain data preprocessor. This allows the model to consider the effects of surface and elevated sources and also differentiation of simple and complex terrains [22].

In order to evaluate the impact on air quality due to emissions from the coke handling and storage system, the region where the RNEST oil refinery (in the northeastern of Brazil) was installed was selected. This refinery is located in a region with areas of ecological

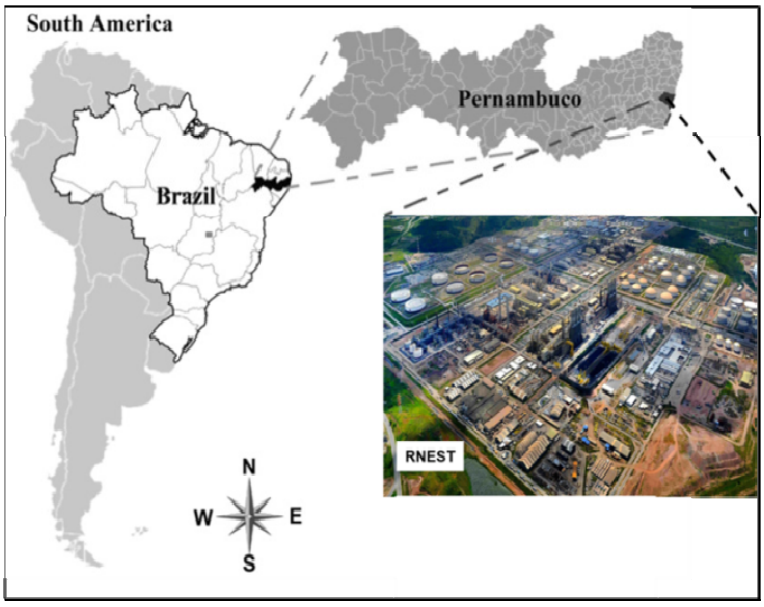

Fig. 1 Geographical location of the selected region for the case study.

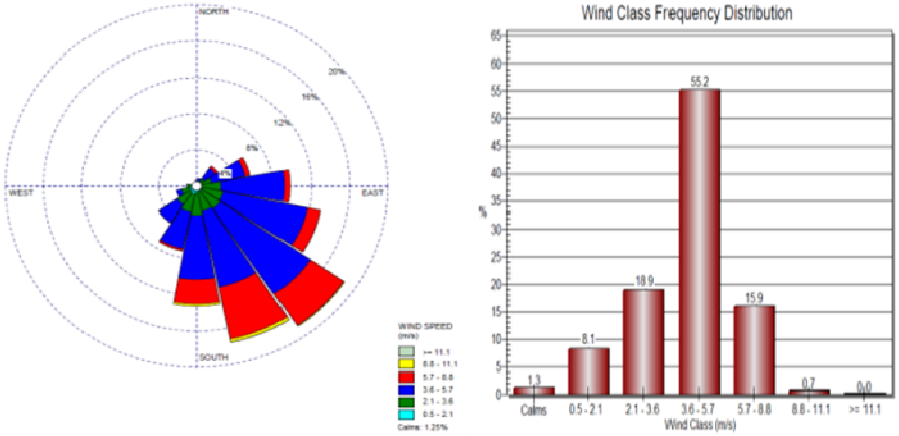

Fig. 2 Wind rose and wind class frequency distribution of three-year period (2006-2008) for the region select for analysis.

preservation and a seaside resorts with great tourist attractiveness, making this region a sensitive area where the impacts should be the minimum possible. Fig. 1 shows the localization of the selected region.

RNEST oil refinery is located in Ipojuca, state of Pernambuco, in the Suape Port Industrial Complex, 45 km away from Recife.

This site is a flatland region with low density of construction and building, the terrain data were obtained from Geographic Information System Resource (Web GIS, 2015) global 3 arc-sec data (SRTM3) with an approximate resolution of 90 by 90 m. The local meteorological data were the same as those used for atmospheric dispersion studies during the refinery developments phase. The data series covers a three-year period (2006-2008). Fig. 2 shows the wind rose and the wind class frequency distribution for the period mentioned.

To register the emission sources of the coke handling and storage system in the modelling software the most significant ones were selected: (i) cokepit/cokepad area; (ii) hopper; (iii) conveyors belts; (iv) transfer points; (v) coke stockpiles; (vi) trucks bucket. Each of these sources was registered according to their physical characteristics that most influence the dispersion process of the pollutants. The cokepit/cokepad area,

hopper and trucks bucket were characterized as area source; the transfer points as point source; the conveyors belts as line-volume and the coke stockpiles as volume source. The pollutant analyzed was PM_{10} and deposition effect was not considered in this study. The isoconcentration curves of the pollutants were defined with a Cartesian grid for the receptors with spacing of 500 m resulting in an analysis region with 17 km of extension in the X axis and 20.5 km in the Y axis, from the central point located in the coordinates 8º22'36.80" S latitude and 35º0'28.96" O longitude.

3 Results and Discussion

3.1 Emissions Results

Mechanic system (scenario 3) has the highest emission rates, followed by semi-automated system (scenario 2) and automated system (scenario 1), as can be seen in the graph shown in Fig. 3.

The source that most contributes to system emissions is the wheel loader, the vehicle moving around the stockpile area is the second largest. A justification for emission increase deriving from wheel loaders use or vehicle circulation on piles corresponds to an increase on material breakage and consequently in the present silt content. In the calculations, the value of 5% was kept for silt content, since it was considered that the increase in silt content would be computed in the equation used to estimate emissions from these activities. Adoption of control measures, such as the ones listed in Table 1, reduces 50% on average of the total emission emitted for each scenario. However, by comparing the emissions of scenario 1 with those of scenarios 2 and 3, it is observed that the non-use of the wheel loader for the handling and storage of coke provides emission values smaller than those of the scenarios that consider the use of this equipment. This finding indicates that the use of appropriate equipment for the coke handling, such as stackers or reclaimers, is more effective in reducing emissions than the control measures considered in Table 1.

In order to evaluate the influence of PM_{10} emissions from the coke handling and storage system, these were compared with the other PM emissions from the refinery. For this comparison, it was considered a refinery without the FCC unit, considering that the PM emission sources would result from furnaces and boilers of the process units and also from the flare system. By analyzing the three scenarios with the

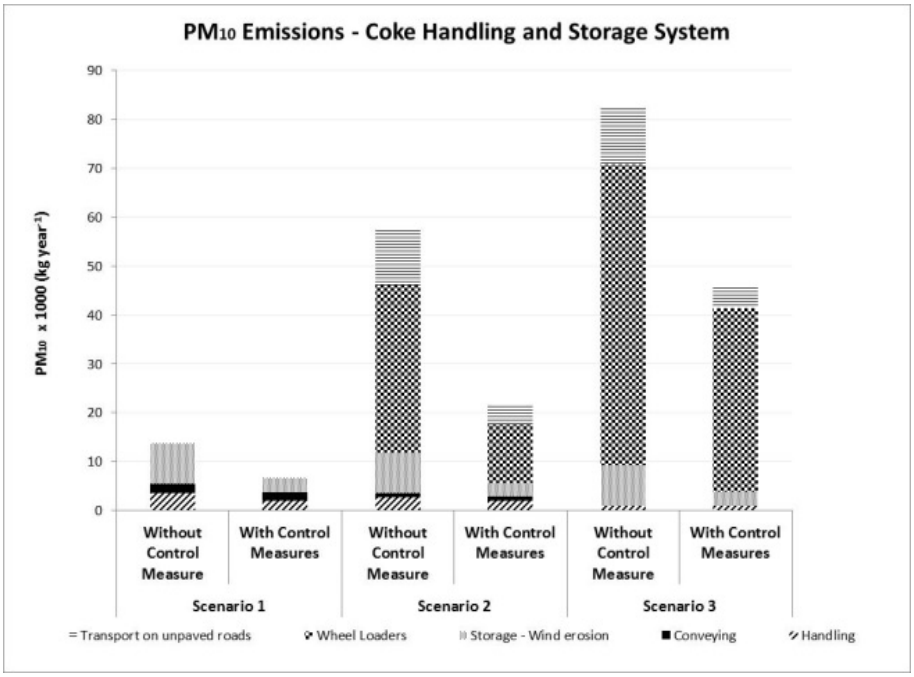

Fig. 3 PM_{10} emissions related to the handling and storage of petroleum coke system for the three scenarios studied.

implementation of control measures, it can be concluded that emissions in handling and storage petroleum coke system represent only 11% of total emissions for scenario 3, which has the highest emission. For scenario 1, that is, the one with the highest automation level, system emissions correspond to only 2% of the total. In the evaluation carried out by Ref. [23] PM_{10} emissions from coke handling system correspond to only 3% of PM_{10} emissions of a DCU, the remainder comes from coke furnaces. Such information ratifies the finding that the PM_{10} emissions of coke handling system are small compared to the total emitted by the refinery.

This distinction between emission sources, allows us to know the real impact of the handling and coke storage system compared with remaining refinery emissions. Handling and storage of a solid product brings a great visual impact and can give a false idea of a significant contribution for PM_{10} emissions. Studies concerned with emission reduction in the storage area comprehend several fronts: shape of piles in the storage area, for instance, can influence PM emission for the same location, as well as the number of piles in a patio [24-26], the length-height relation of piles [27] and the localization of them in comparison with the incidence angle of predominant winds [28]. Despite the studies previously mentioned, the technology most utilized in PM emissions reduction, is the installation of a cover for the storage area. The coverage is certainly the most efficient measure, since it eliminates wind action on the piles and reduces drastically the system's emissions, however it brings additional damage to it, such as the risk of explosion, which needs special care, besides the high cost for its implementation. The use of windbreaks, has been shown an advantageous option and does not harm the system's operational safety, even though it also needs a considerable investment for its installation. The Australian Agency technical guide recommends considering an emission reduction of 30% when the windbreaks are used. Nevertheless, the studies carried out by Turpin, C., et al. [29] showed that reduction values up to 85% can be reached when the whole patio is surrounded by windbreaks. Regarding transfer operations, conveyor transfer stations are the ones that draw most attention due to the high potential of dusts emission. For this reason, most conveyor transfer stations are usually confinement, but this might bring an extra safety concern, it increases the risk of explosion. Studies performed by Cong, X. C., et al. [30] point out that the main parameters that influence dusts generation during transfer are height of fall and material temperature during transfer. Configurations of conveyor transfer stations also influence the quantity of emitted dusts according to studies carried out by Wypych, P., et al. [31].

3.2 Atmospheric Dispersion Modelling Study

The results of the atmospheric dispersion study presented the same behavior as the emission rate analysis: the most automated system presented the lowest concentrations of PM_{10} and the mechanical system the highest ones. Fig. 4 illustrates a comparison of the maximum concentrations obtained with the air quality standards of United States and European Community. It is important to remark that the European Union standards are the same as those recommended by the World Health Organization for the maximum concentration for the 24-h period.

Among the analyzed scenarios, the mechanic is the only one whose maximum PM_{10} concentration surpasses the European Air Quality standard. However, this standard allows the value of 35 times a year to be surpassed. According to the atmospheric dispersion study performed, the value of 50 $\mu g/m^3$ is surpassed only 10 times in 3 years of analysis. Consequently, even the handling and coke storage system, with lower automation level, does not present major impact in air quality. The semi-automated configuration has its maximum concentrations below the value stipulated by the European legislation, which is the most restrictive one, as well as the scenario with the most automated configuration. The three scenarios analyzed have

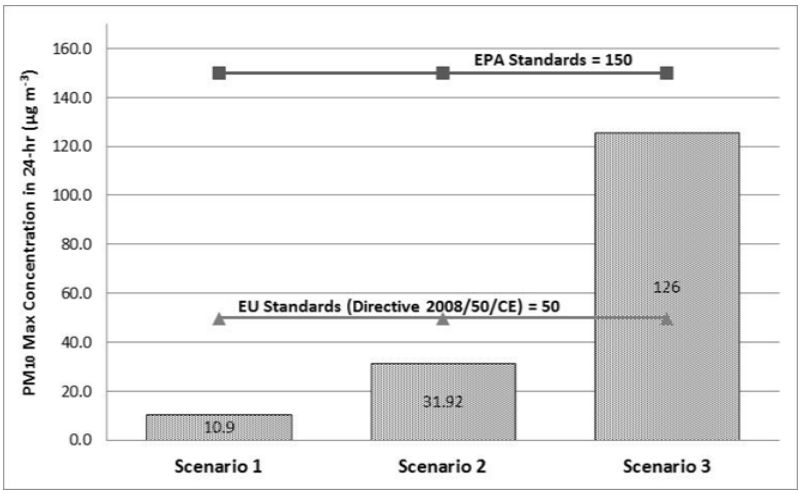

Fig. 4 Comparison of the highest PM_{10} concentration for the 24-h period of each scenario and the main air quality standards.

maximum concentration values below the American standard. Another important aspect to be analyzed is the plume behavior observed in the dispersion study. For the three scenarios, the maximum concentration point is very close to the emission sources, but as it distances from the sources, PM_{10} concentrations reduce very quickly. Out of the considered refinery limits, concentration values are lower than those established by the air quality standards, even for those more restrictive.

The results of the atmospheric dispersion study show and refer only to the coke handling and storage system, considering the control measures presented in Table 1. For air quality purposes, the total emissions from the refinery should be considered. However, the objective of this work was to identify the impact of the coke handling and storage system on PM emissions. For this reason only the PM_{10} emissions from the coke handling and storage system were analyzed.

4. Conclusion

The results obtained from this work indicated that the higher the automation level in handling and coke storage system, lower are the PM_{10} emissions. The main advantage is in avoiding wheel loaders for pile formation and/or removal of the coke from storage area. Truck loading using silos also favors emission reduction, as there are no vehicles moving in storage area. Among the operations present in an automated system, the most significant for emissions is outdoors material storage. That is the reason why the most important control measures are during this phase. However, the remaining operations, such as transfers, cannot be neglected.

Handling and coke storage system emissions represent a low percentage of the total PM_{10} emissions in a oil refinery, as it is found between 11% and 2% depending on the analyzed system configuration. These evaluations are important to aid in the investment decision process to mitigate PM_{10} emissions in a petroleum refinery. Since the contribution of such system does not represent a significant portion of the total, investments will have a high cost-effectiveness relationship and efforts and investments must firstly be directed to sources with higher emission potential and greater contribution in global analysis. This must be one of the reasons why a great part of handling and coke storage systems are not totally automated.

Regarding the results of the atmospheric dispersion study, it can be observed that the PM_{10} emissions are more concentrated close to sources. Probably, this is due to characteristics of the emission sources, although the meteorological and topography data also contribute to the result of pollutants dispersion.

Acknowledgements

The authors thank PETROBRAS, for the data support to this research.

References

[1] Stanek, L. W., Sacks, J. D., Dutton, S. J., and Dubois, J.-J. B. 2011. "Attributing Health Effects to Apportioned Components and Sources of Particulate Matter: An Evaluation of Collective Results." *Atmospheric Environment* 45: 5655-63.

[2] Tabaku, A., Bejtja, G., Bala, S., Toci, E., and Resuli, J., 2011. "Effects of Air Pollution on Children's Pulmonary Health." *Atmospheric Environment* 45: 7540-5.

[3] EC. 2008. "Relating to Ambient Air Quality and Cleaner Air for Europe." Directive 2008/50/EC of the European Parliament and of the Council.

[4] U.S. EPA (United States Environmental Protection Agency). 2015. Particulate Matter PM Standards—Table of Historical PM NAAQS. http://www.epa.gov/ttn/naaqs/standards/pm/s_pm_history.html.

[5] WHO (World Health Organization). 2006. Air Quality Guidelines—Global Update 2005. "Particulate Matter, Ozone, Nitrogen Dioxide and Sulfur Dioxide." Regional Office for Europe.

[6] Karagulian, F., Belis, C. A., Dora, C. F. C., Prüss-Ustün, A. M., Bonjour, S., Adair-Rohani, H., and Amann, M. 2015. "Contribuitons to Cities' Ambient Particulate Matter (PM): A Systematic Review of Local Source Contributions at Global Level." *Atmospheric Environment* 120: 475-83.

[7] Puliafito, S. E., Castro, F., and Allende, D. 2011. "Air-Quality Impact of PM_{10} Emission in Urbancentres." *International Journal of Environment and Pollution* 46: 127-43.

[8] Winiwarter, W., Kuhlbusch, T. A. J., Viana, M., and Hitzenberger, R. 2009. "Quality Considerations of European PM Emission Inventories." *Atmospheric Environment* 43: 3819-28.

[9] Szklo, A. S. 2005. "A Refinaria de Petróleo-Impactos Ambientais." In *Fundamentos do Refino do Petróleo*, edited by A. S. Szklo. Rio de Janeiro: Interciência, 76-82.

[10] Ekmann, J. M., and Le, P. H. 2004. "Coal Storage and Transportation." *Encyclopedia of Energy* 551-80.

[11] Bohn, R., Cuscino, T. Jr., and Cowherd, C. Jr. 1978. "Fugitive Emissions from Integrated Iron and Steel Plants' EPA-600/2-78-050." United States Environmental Protection Agency.

[12] NPI (National Pollutant Inventory). 2012. "Emission Estimation Technique Manual for Mining." Version 3.1, Australian Government.

[13] EEA (European Environment Agency). 2013. "EMEP/EEA Air Pollutant Emission Inventory Guidebook 2013. Technical Guidance to Prepare National Emission Inventories." http://www.eea.europa.eu/publications/emep-eea-guidebook-2013.

[14] Martín, F., Pujadas, M., Artiñano, B., Gómez-Moreno, F., Palomino, I., Moreno, N., et al. 2007. "Estimates of Atmospheric Particle Emissions from Bulk Handling of Dusty Materials in Spanish Harbours." *Atmospheric Environment* 41: 6356-65.

[15] Monfort, E., Sanfélix, V., Celades, I., Gomar, S., Martín, F., Aceña, B., and Pascual, A. 2011. "Diffuse PM_{10} Emission Factors Associated with Dust Abatement Technologies in the Ceramic Industry." *Atmospheric Environment* 45: 7286-92.

[16] U.S. EPA (United States Environmental Protection Agency). 2006. "AP 42-Compilation of Air Pollutants Emission Factors—Volume I Section 13.2: Introduction to Diffuse Dust Sources." http://www.epa.gov/ttn/chief/ap42/ch13/index.html.

[17] TCEQ (Texas Commission on Environmental Quality). 2008. "NRS Guidance for Petroleum Coke Storage and Transfer—Emissions Calculations."

[18] US EPA (United States Environmental Protection Agency). 1985. "AP 42-Compilation of Air Pollutants Emission Factors—Volume I: Stationary Point and Sources Area." http://www.epa.gov/ttn/chief/ap42/oldeditions.html.

[19] U.S. EPA (United States Environmental Protection Agency). 1998. "AP 42-Compilation of Air Pollutants Emission Factors—Volume I Section 11.9: Western Surface Coal Mining." http://www.epa.gov/ttn/chief/ap42/ch11/index.html.

[20] API (American Petroleum Institute). 2014. Guidance Document for the Storage and Handling of Petroleum Coke.

[21] BREF. 2006. "Reference Document on Best Available Techniques on Emissions from Storage-BREF." European Commission.

[22] RTI. 2015. "Emission Estimation Protocol for Petroleum Refineries." Prepared for U.S. Environmental Protection Agency by Research Triangle Institute, Office of Air Quality Planning and Standards, Research Triangle Park, NC.

[23] U.S. EPA (United States Environmental Protection Agency). 2015b. Technology Transfer Network-SCRAM-Air Quality Models-Dispersion Modeling, http://www3.epa.gov/ttn/scram/dispersionindex.html

[24] Chaplin, D., Wodnik, R., Leung, V., and Ladd, D. 2013.

"Delayed Coking Design for Stringent Environmental Requirements." Presented at the 18th ERTC Annual Meeting. Budapest, Hungary.

[25] Toraño, J., Rodriguez, P., Diego, I., Rivas, J. M., and Pelegry, A. 2007. "Influence of the Pile Shape on Wind Erosion CFD Emission Simulation." *Applied Mathematical Modelling* 31: 2487-502.

[26] Diego, I., Pelegry, A., Torno, S., Toraño, J., and Menendez, M. 2009. "Simultaneous CFD Evaluation of Wind Flow and Dust Emission in Open Storage Piles." *Applied Mathematical Modelling* 33: 3197-207.

[27] Cong, X. C., Cao, S. Q., Chen, Z. L., Peng, S. T., and Yang, S. L. 2011. "Impact of the Installation Scenario of Porous Fences on Wind-Blown Particle Emission in Open Coal Yards." *Atmospheric Environment* 45: 5247-53.

[28] Badr, T., and Harion, J.-L. 2007. "Effect of Aggregate Storage Piles Configuration on Dust Emissions." *Atmospheric Environment* 41: 360-8.

[29] Turpin, C., and Harion, J.-L. 2009. "Numerical Modelling of Flow Structures over Various Flat-Topped Stockpiles Height: Implications on Dust Emissions." *Atmospheric Environment* 43: 5579-87.

[30] Cong, X. C., Yang, S. L., Cao, S. Q., Chen, Z. L., Dai, M. X., and Peng, S. T. 2012. "Effect of Aggregate Stockpile Configuration and Layout on Dust Emissions in an Open Yard." *Applied Mathematical Modelling* 36: 5482-91.

[31] Wypych, P., Cook, D., and Cooper, P. 2005. "Controlling Dust Emissions and Explosion Hazards in Powder Handling Plants." *Chemical Engineering Processing* 44: 323-6.

Journal of Environmental Science and Engineering A 7 (2018) 159-171
doi:10.17265/2162-5298/2018.04.002

Autohydrolyzed Low-Cost Biomass and Adsorbent Aging

Odysseas Kopsidas
Department of Industrial Management and Technology, University of Piraeus, Piraeus 18534, Greece

Abstract: Autohydrolysis or self-hydrolysis or hydrothermal treatment of lignocellulosic materials like sawdust and straw is already used in bioethanol industry for water soluble fermentable sugars production. The main idea in this paper is the use of the autohydrolysis and other thermochemical treatments' solid residue as an adsorbent. In this study continuous fixed-bed-column systems were investigated. Continue-flow experiments were carried out on stainless steel columns with dimensions 15 × 2.5 and 25 × 2.5 cm. In chemical processing, a packed bed is a hollow tube, pipe, or other vessel that is filled with a packing material.

Key words: Autohydrolysis, adsorption, desorption, biomass, MB (Methylene Blue).

1. Introduction

In fact, the adsorbent is the solid by-product in the fermentable sugars production by autohydrolysis. Autohydrolysis of lignocellulosic materials can be used as a first step while enzymatic or acid hydrolysis is usually used as second step in the bioethanol industry. Many industries, such as paper, plastics, food, printing, leather, cosmetics and textile, use dyes in order to color their products [1]. In textile industries, about 10-15% of the dye gets lost in the effluent during the dyeing process which are harmful products and may cause cancer epidemics [2, 3]. Dyes usually have a synthetic origin and complex aromatic molecular structures which make them more stable and more difficult to biodegrade [1-4]. In wastewater treatment, various methods applied to remove dyes include photocatalytic degradation [5, 6], membrane separation [7], chemical oxidations [8] and electrochemical process. Among the above mentioned techniques of dye removal, the process of adsorption gives the best results as it can be used to remove different types of coloring materials [9]. Adsorption onto activated carbon is the most widespread technology for the removal of pollutants from water and wastewaters.

The adsorbents which authors use are: spruce (*Picea abies*) untreated, spruce modified by autohydrolysis, wheat straw untreated, barley straw untreated, lentil straw untreated, chickpeas straw untreated and algae untreated. The column systems were filed with biomass at various initial dye concentrations, flow rates and bed-depths. The column kinetics of MB (Methylene Blue) adsorption on spruce (*Picea abies*) untreated, spruce modified by autohydrolysis, wheat straw untreated, barley straw untreated, lentil straw untreated, chickpeas untreated, algal untreated biomass, was simulated herein, using biomass as control, in order to facilitate its potential use as a low-cost adsorbent for wastewater dye removal. Economies arise when the facility that can use such adsorption materials is near a source of a lignocellulosic waste as agricultural residues, thus saving transportation cost and contributing to industrial ecology at local level.

2. Materials and Methods

2.1 Materials

The Scots pine (*Pinus sylvestris L.*) sawdust used was obtained from a local furniture manufacturing

Corresponding author: Odysseas Kopsidas, Ph.D., research field: environmental economics.

company, as a suitable source for full-scale/industrial applications. The moisture content of the material when received was 8.7% (w/w); after screening, the fraction with particle sizes between 0.2 and 1 mm was isolated. The composition of the raw material was as follows (expressed in % w/w on a dry weight basis): 40.1% cellulose measured as glucan (with 52.5% XRD (X-Ray Diffraction) degree of crystallinity); 28.5% hemicelluloses (16.0% measured as manan, 8.9% measured as xylan and the rest 3.6% measured as arabinan); 27.7% Klason acid-insoluble lignin, 0.2% ash, and 3.5% extractives and other acid soluble components (e.g. acid soluble lignin). The spruce (*Picea Abies*) sawdust used was obtained from a local furniture manufacturing company, as a suitable source for full-scale/industrial applications. The moisture content of the material when received was 9% (w/w); after screening, the fraction with particle sizes between 0.2 and 0.9 mm was isolated. Wheat straw (*Triticum aestivum*) obtained from Thessaly in Central Greece had a moisture content of 8.75% w/w. It was chopped with hedge shears in small pieces and the fraction with sizes 1-2 cm (representing more than 95% of the raw total wheat straw) was collected by sieving. This fraction was chosen because it is more suitable for scale up of the process.

Barley straw (*Hordeum vulgare*) used was obtained from Thessaly (Central Greece), as a suitable source for full-scale/industrial applications. Barley straw contains 27% w/w hemicelluloses, 33% w/w cellulose, lignin 28% w/w and 12% w/w ash. The moisture of the material measured was 8.5% w/w. After grinding in a hummer mill and screening, the fraction with particle sizes between 1 and 2 cm was isolated as “coarse grinded barley straw”. The material was saturated for 24 hours prior to adsorption experiments. The moisture of the barley straw was 8.5% w/w. After grinding by a hummer mill and screening, the fraction with particle sizes between 1.5 and 2.5 cm was isolated as “coarse grinded barley straw”. It was saturated for 24 hours before the experimental procedure. The lentil straw (*Lens culinaris)* is an edible pulse. It is a bushy annual plant of the legume family, grown for its lens-shaped seeds. It is about 40 centimeters (16 in.) tall and the seeds grow in pods, usually with two seeds in each. Lentils have been part of the human diet since the aceramic (before pottery) Neolithic times, being one of the first crops domesticated in the Near East. Archeological evidence shows they were eaten 9,500 to 13,000 years ago. Lentil colors range from yellow to red-orange to green, brown and black. Lentils also vary in size and are sold in many forms, with or without the skins, whole or split.

The chickpeas straw is from a plant which grows to between 20-50 cm (8-20 inches) high and has small feathery leaves on either side of the stem. Chickpeas are a type of pulse, with one seedpod containing two or three peas. It has white flowers with blue, violet or pink veins. Chickpeas need a subtropical or tropical climate with more than 400 millimetres (16 in.) of annual rain (citation needed) They can be grown in a temperate climate but yields will be much lower.

Algae (*Microcystis*, *Cyclotella*, *Cryptomonas* and *Scenedesmus*) are a very large and diverse group of simple, typically autotrophic organisms, ranging from unicellular to mu lticellular forms, such as the giant kelp (large brown alga), that may grow up to 50 meters in length. Most are photosynthetic and “simple” because they lack many of the distinct cell organelles and cell types found in land plants. The largest and most complex marine forms are called seaweeds. Wood chips are a medium-sized solid material made by cutting, or chipping, larger pieces of wood. Woodchips may be used as a biomass solid fuel and are raw material for producing wood pulp. They may also be used as an organic mulch in gardening, landscaping, restoration ecology and mushroom cultivation. According to the different chemical and mechanical properties of the masses, the wood logs are mostly peeled, and the bark chips and the

woodchips processed in different processes. Wood chips used for chemical pulp must be relatively uniform in size and free of bark. The optimum size varies with the wood species. It is important to avoid damage to the wood fibres as this is important for the pulp properties. For round wood, it is most common to use disk chippers. A typical size of the disk is 2.0-3.5 m in diameter, 10-25 cm in thickness and weight is up to 30 tons. The disk is fitted with 4 to 16 knives and driven with motors of ½-2 MW. Drum chippers are normally used for wood residuals from saw mills or other wood industry.

MB (CI 52015) is a heterocyclic aromatic chemical compound with the molecular formula $C_{16}H_{18}N_3SCl$. It has many uses in a range of different fields, such as biology and chemistry. At room temperature it appears as a solid, odorless, dark green powder that yields a blue solution when dissolved in water. The hydrated form has 3 molecules of water per molecule of MB. MB should not be confused with methyl blue, another histology stain, new MB, nor with the methyl violets often used as pH indicators. As an experimental pharmaceutical drug, the INN (International Nonproprietary Name) of MB is methylthioninium chloride. MB was first prepared in 1876 by German chemist Heinrich Caro (1834-1910). The formation of MB after the reaction of hydrogen sulfide with dimethyl-p-phenylenediamine and iron(III) at pH 0.4-0.7 is used to determine by photometric measurements sulfide concentration in the range 0.020 to 1.50 mg/L (20 ppb to 1.5 ppm). The test is very sensitive and the blue coloration developing upon contact of the reagents with dissolved H_2S is stable for 60 min. Ready-to-use kits such as the Spectroquant sulfide test [8] facilitate routine analyses. The MB sulfide test is a convenient method often used in soil microbiology to quickly detect in water the metabolic activity of SRB (Sulfate Reducing Bacteria). It should be observed that in this test, MB is a product of reaction and not a reagent.

The addition of a strong reducing agent, such as ascorbic acid, to a sulfide-containing solution is sometimes used to prevent sulfide oxidation from atmospheric oxygen. Although it is certainly a sound precaution for the determination of sulfide with an ion selective electrode, it might however hamper the development of the blue color if the freshly formed MB is also reduced, as described here above in the paragraph on redox indicator.

2.2 Pretreatment

The autohydrolysis process was performed in a 3.75-L batch reactor PARR 4843. The isothermal autohydrolysis time was tai = 0, 10, 20, 30, 40 and 50 min (not including the non-isothermal preheating and the cooling time-periods); the reaction was catalyzed by the organic acids produced by the pine sawdust itself during autohydrolysis at a liquid-to-solid ratio of 10:1; the liquid phase volume (water) was 2,000 mL and the solid material dose (pine sawdust) was 200 g; stirring speed 150 rpm. The reaction ending temperature values were T = 160 °C, 200 °C and 240 °C, reached after t = 42, 62 and 80 min preheating time values, respectively. The autohydrolysis product was filtered using a Buchner filter with Munktell paper sheet (grade 34/N) to separate the liquid phase from the solid phase. The solid residue was washed with water until neutral pH (the initial filtrate pH was 2.90-4.76 depending on the autohydrolysis severity). The solid residue was dried at 110 °C for 10 days at room temperature to reach the humidity of the untreated material. Then it was used as adsorbent.

2.3. Continuous Fixed-Bed Column Studies

Continue-flow experiments were carried out on stainless steel columns with dimensions 15 × 2.5 and 25 × 2.5 cm. The bed height was x = 15 cm and 25 cm, respectively. The adsorbent weight was m = 32 g and 54 g, respectively. The pH was 8.0. The flow rates were fixed at approximately 20 and 40 $mL \cdot min^{-1}$ using a preparative HPLC (High Performance Liquid Chromatography) pump, LaPrep P110-VWR-VWR

International. The initial concentrations of MB were 160, 80 and 40 mg·L^{-1}. To determine the concentration of MB in the effluent, samples of outflow were peaked at 100 mL intervals. At the end of each one of the above mentioned sorption experiments, desorption tests were performed using distilled water as influent. The flow rate was fixed at about 20 mL·min^{-1}. To determine the concentration of MB in the effluent, samples of outflow were collected at 100 mL intervals.

3. Results and Discussion

3.1 Continuous Fixed-Bed-Column Adsorption Model

A widely used continuous fixed-bed-column model was established by Bohart and Adams, who assumed that the rate of adsorption is controlled by the surface binding (through chemical reaction or physical interaction) between adsorbate and unused capacity of the solid, i.e., adsorption rate = KCC_u, where K is the adsorption rate coefficient, C is the adsorbate concentration at the solid phase at distance x, and C_u is the unused surface adsorptive capacity at time t, expressed as mass per volume of bed. The material balance for adsorbate is given by the partial differential equation:

$$\frac{\partial C_u}{\partial t} = -K \cdot C \cdot C_u \quad (1)$$

while the corresponding partial differential equation for the C_u decrease is

$$\frac{\partial C}{\partial x} = -\frac{K}{u} \cdot C \cdot C_u \quad (2)$$

where u is the superficial liquid velocity. These equations are obtained neglecting diffusion and accumulation terms, with assumptions that are valid in chemical engineering practice, provided that strict scale up specifications are kept in the design stage and successful operation conditions are kept in the industrial operation stage.

The differential equations can be integrated over the total length x of the bed to give:

$$\ln\left(\frac{C_i}{C} - 1\right) = \ln\left[\exp\left(\frac{K.N.x}{u}\right) - 1\right] - K \cdot C_i \cdot t \quad (3)$$

where N (mg·L^{-1}); is the initial or total adsorption capacity coefficient, also quoted as $C_{u,0}$ [9, 10]; C = effluent concentration (mg·L^{-1}); C_i = influent concentration (mg·L^{-1}); K = adsorption rate coefficient ($L \cdot mg^{-1} \cdot min^{-1}$); x = bed depth (cm); u = linear velocity (cm·min^{-1}); and t = time (min). Since $\exp(K.N.x/u)$ is usually much greater than unity, this equation can be simplified to:

$$\ln\left(\frac{C_i}{C} - 1\right) = \frac{K \cdot N \cdot x}{u} - K \cdot C_i \cdot t \quad (4)$$

which is commonly used by researchers, because of its convenience in estimating the values of parameters K and N through linear regression either of $\ln[(C_0/C_i) - 1]$ vs. t or t vs. x when the following rearrangement is adopted:

$$t = \frac{N \cdot x}{C_i \cdot u} - \frac{1}{K \cdot C_i} \cdot \left(\ln\frac{C_i}{C} - 1\right) \quad (5)$$

In this rearrangement, t is the time to breakthrough, i.e., the time period required for concentration to reach a predetermined value. For using the last expression as a linear regression model, wastewater is passed through beds of varying depths, keeping constant C_i and u, preferably at values similar to those expected to prevail under real conditions at full scale. Alternatively, it can be performed by the aid of at least three columns arranged in series. In such a case, sampling takes place at the bottom of each column and is measured for adsorbate concentration, making more frequent measurements when approaching the breakthrough concentration C. Finally, the time at which the effluent reaches this concentration is used as the dependent variable while x plans the role of the independent one. Evidently, the use of such a regression model implies the additional error of measuring the independent variable with less precision

in comparison with the dependent. The common error in both models comes from the estimation of concentration from measuring adsorbance although the reference relation/curve has been structured/drawn in the inverse mode, i.e., for predetermined concentrations the corresponding adsorbances have been measured.

In the present work, the model of Eq. (5) has been used for parameter values estimation through linear regression to obtain numerical results compared with corresponding data found for other fixed bed adsorption studies in literature. The non-linear form of this model is:

$$C = \frac{C_i}{1 + Ae^{-rt}} \tag{6}$$

where $A = e^{K \cdot N \cdot x / u}$; $r = K \cdot C_i$.

On the other hand, Clark has advanced the Bohart and Adams model by incorporating the parameter n of the Freundlich adsorption isotherm:

$$C = \left[\frac{C_i^{n-1}}{1 + Ae^{-rt}} \right]^{\frac{1}{n-1}} \tag{7}$$

where n = inverse of the slope of the Freundlich isotherm. Finally, the Bohart and Adams model can be reduced for $n = 2$ from Clark model.

3.2 Continuous Fixed-Bed-Column Desorption Model

The kinetic equation used for desorption is Eq. (8):

$$C = C'_0 \, e^{-k' \cdot t'} \tag{8}$$

where C'_0 is the initial MB concentration of desorption effluent, k' is desorption rate constant assuming first order desorption kinetics and t' is desorption time.

3.3 Fixed-Bed Column Results for MB Adsorption on Lignocellulosic Biomass

The packing can be randomly filled with small objects like Raschig rings or else it can be a specifically designed structured packing. Packed beds may also contain catalyst particles or adsorbents such as zeolite pellets, granular activated carbon, etc.. The purpose of a packed bed is typically to improve contact between two phases in a chemical or similar process. Packed beds can be used in a chemical reactor, a distillation process, or a scrubber, but packed beds have also been used to store heat in chemical plants. In this case, hot gases are allowed to escape through a vessel that is packed with a refractory material until the packing is hot. Air or other cool gas is then fed back to the plant through the hot bed, thereby pre-heating the air or gas feed. The Ergun equation can be used to predict the pressure drop along the length of a packed bed given the fluid velocity, the packing size, and the viscosity and density of the fluid.

The values of parameters A and r according to the Bohart and Adams model were estimated by LRA (Linear Regression Analysis) from the column effluent data for all the cases. The expressions used to calculate the parameter K and N values after having performed LRA are $K = r/C_i$ and $N = u \cdot lnA/(x \cdot K) = C_i \cdot u \cdot lnA/(x \cdot r)$. The effluent dye solution volume V (in L) is $V = Qt$, where Q is the dye solution flow rate. The theoretical estimations, according to the Bohart and Adams model, the N and K values are presented in Tables 1-9.

The effects of initial MB concentration have been investigated at 40-160 $g \cdot L^{-1}$, respectively. The bed height was 15 cm and the temperature was 23 °C. The flow rate was fixed at 20 $mL \cdot min^{-1}$ and the pH of MB solution was 8. The breakthrough curves were plotted in figures (Figs. 1-20) according to the Bohart and Adams model. Flow rate is one of the most important characteristics in evaluating sorbents for continuous treatment of dyes effluents on an industrial scale [9, 10]. The effect of flow rate in the fixed bed column, packed with biomass, was investigated varying the flow rate from 10-40 $mL \cdot min^{-1}$ with bed depths held constant at 15 cm. The pH was 8. The influent MB

Table 1 Fixed bed column systems for spruce.

C_i	Q (mL/min)	x (cm)	m (g)	N	K	R	q_o (mg/g)
160	20	15	12	6,683	0.000318	-0.9506	40.99
160	20	15	12	7,400	0.000100	-0.9367	45.38
160	20	15	13	6,507	0.000356	-0.9992	36.84
160	20	15	13	6,387	0.000518	-0.9539	36.16
160	20	15	13	6,387	0.000518	-0.9539	36.16
160	20	15	15	5,329	0.000416	-0.9153	26.14
160	20	15	19	5,274	0.000415	-0.9457	20.16
160	20	15	19	5,274	0.000415	-0.9457	20.16
160	20	15	20	9,248	0.000110	-0.9530	19.19
160	20	15	20	8,738	0.000216	-0.9765	32.15
160	40	15	20	4,459	0.000515	-0.9903	16.41
160	40	25	34	5,320	0.000347	-0.9892	19.19
160	20	25	34	6,154	0.000243	-0.9870	22.20
80	40	25	34	4,480	0.000689	-0.9911	16.16

Table 2 Fixed bed column systems for spruce modified by autohydrolysis (x = 15 cm).

T (^{o}C)	t (min)	Ci	Q (mL/min)	m (g)	N	K	R	q_o (mg/g)
160	0	160	20	16.5	9,643	0.000146	-0.9313	43.01
160	0	160	20	16.5	6,492	0.000541	-0.9651	28.96
160	20	160	20	16.5	6,362	0.000449	-0.9573	28.38
160	30	160	20	16.5	7,176	0.000381	-0.9325	32.01
160	40	160	20	16.5	6,092	0.000596	-0.9779	27.17
160	50	160	20	16.5	10,412	0.000193	-0.8966	46.44
180	10	160	20	16.5	6,926	0.000371	-0.9740	30.89
240	30	160	20	13.81	7,355	0.000229	-0.9551	41.06
240	50	160	20	14.16	5,389	0.000275	-0.9813	28.38

Table 3 Fixed bed column systems for pine (x = 15 cm).

T (°C)	t (min)	C_i	Q (mL/min)	m (g)	N	K	R	q_o (mg/g)
240	50	178	21	14.16	6,374	0.000220	-0.7944	25.87
		178	21	14.16	6374	0.000220	-0.7944	25.87

Table 4 Fixed-bed column systems for wheat straw.

C_i	Q (mL/min)	x (cm)	m (g)	N	K	R	q_o *(mg/g)*
160	20	15	4.4	-3,998	0.000100	-0.9396	6.43
160	40	15	14	-863	0.000083	-0.9245	6.21
160	20	25	22.6	4,053	0.000122	-0.9214	22.42
160	40	25	22.6	4,053	0.000122	-0.9214	22.42

Table 5 Fixed-bed column systems for barley straw.

C_i	Q (mL/min)	x (cm)	m (g)	N	K	R	q_o (mg/g)
160	40	15	20	4,221	0.000646	-0.9651	32.42
20	20	15	14	786	0.000793	-0.9413	6.07
20	20	15	5	72	0.001624	-0.9626	2.49
20	20	15	5	72	0.001624	-0.9626	2.49
160	40	15	20	2,052	0.000115	-0.8606	30.80
20	20	25	21.96	2,395	0.000450	-0.9698	10.90
160	40	15	22.6	6,264	0.000578	-0.9620	24.50

Table 6 Fixed-bed column systems for chickpea straw.

C_i	Q (mL/min)	x (cm)	m (g)	N	K	R	q_o (mg/g)
160	20	15	11	7,537	0.000139	-0.9829	50.43
160	20	15	11	7,559	0.000140	-0.9835	50.58

Table 7 Fixed-bed column systems for lentil straw.

C_i	Q (mL/min)	x (cm)	m (g)	N	K	R	q_o (mg/g)
160	10	15	9.03	5,310	0.00004	-0.9971	43.99
40	20	15	9	2,771	0.00019	-0.9901	22.66
160	10	15	9.03	2,822	0.00005	-0.9122	23.00
160	10	15	9.03	2,871	0.00005	-0.9086	23.40
80	20	25	15	7,666	0.00006	-0.9487	62.69
80	20	25	15	3,491	0.00010	-0.9588	31.24

Table 8 Fixed-bed column systems for algal biomass.

C_i	Q (mL/min)	x (cm)	m (g)	N	K	R	q_o (mg/g)
160	20	15	17	5,017	0.000124	-0.9548	22.76
160	40	25	28	2,509	0.000200	-0.9649	11.81

Table 9 Fixed-bed column systems for woodchips.

C_i	Q (mL/min)	x (cm)	m (g)	N	K	R	q_o (mg/g)
160	20	15	6.5	-1,463	0.000208	-0.7523	6.51
160	20	15	8.6	-4,920	0.000131	-0.9360	4.84
160	40	25	14.6	-1,240	0.000175	-0.9599	5.90

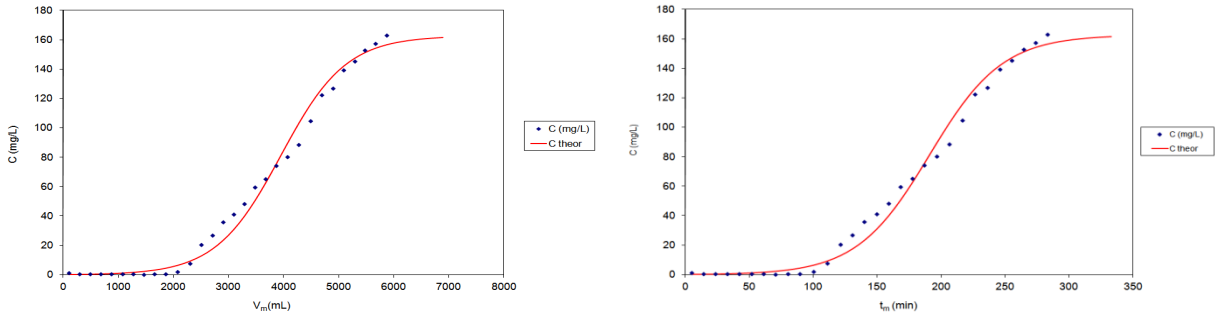

Fig. 1 Column experimental data and theoretical curves of MB adsorption on spruce; the effluent concentration is presented vs. (a) the effluent volume and (b) the adsorption time; x = 15 cm, C_i = 160 mg·L^{-1}, Q = 20 mL·min^{-1} (the theoretical curves are according to the Bohart and Adams model).

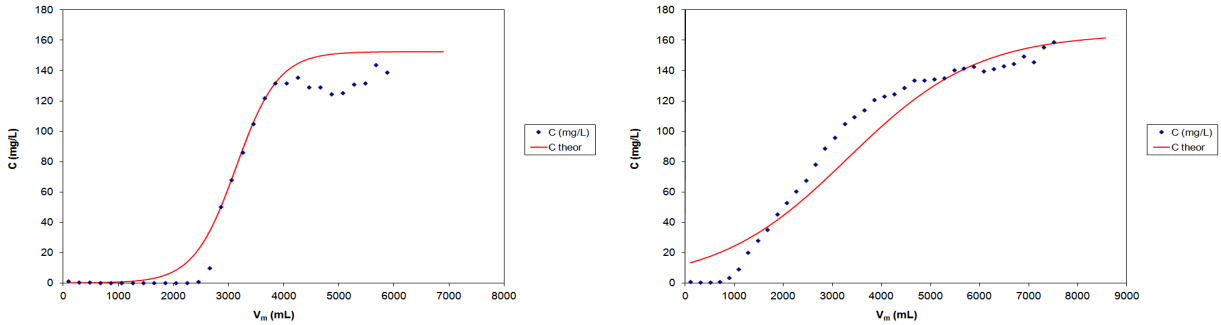

Fig. 2 Column experimental data and theoretical curves of MB adsorption on spruce; the effluent concentration is presented vs. (a) the effluent volume and (b) the adsorption time; x = 15 cm, C_i = 160 mg·L^{-1}, Q = 40 mL·min^{-1} (the theoretical curves are according to the Bohart and Adams model).

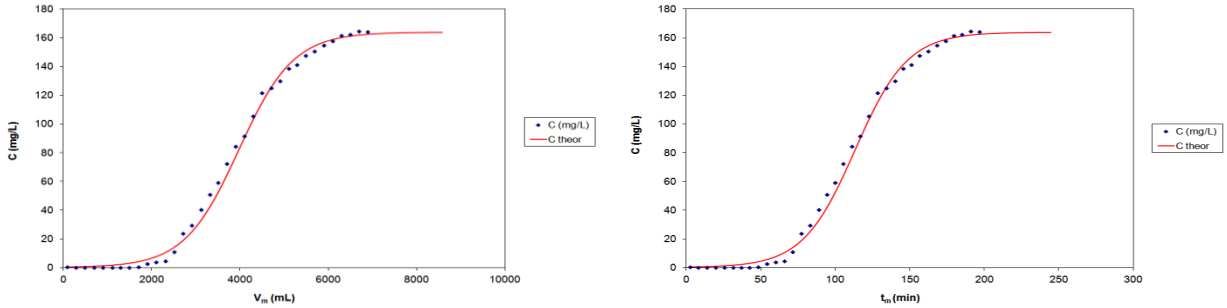

Fig. 3 Column experimental data and theoretical curves of MB adsorption on spruce; the effluent concentration is presented vs. (a) the effluent volume and (b) the adsorption time; x = 25 cm, C_i = 160 mg·L^{-1}, Q = 40 mL·min^{-1} (the theoretical curves are according to the Bohart and Adams model).

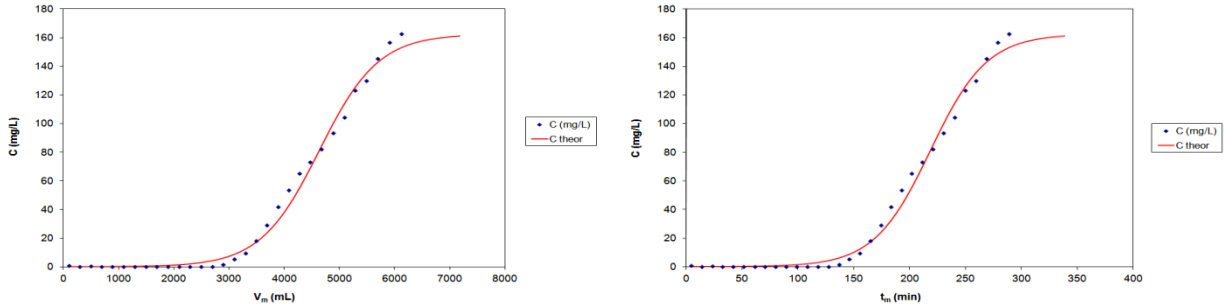

Fig. 4 Column experimental data and theoretical curves of MB adsorption on spruce; the effluent concentration is presented vs. (a) the effluent volume and (b) the adsorption time; x = 25 cm, C_i = 160 mg·L^{-1}, Q = 20 mL·min^{-1} (the theoretical curves are according to the Bohart and Adams model).

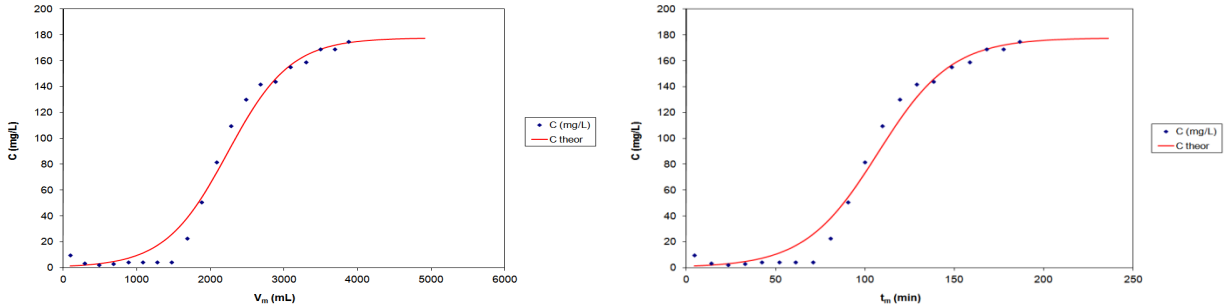

Fig. 5 Column experimental data and theoretical curves of MB adsorption on modified spruce; the effluent concentration is presented vs. (a) the effluent volume and (b) the adsorption time; x = 15 cm, C_i = 160 mg·L^{-1}, Q = 20 mL·min^{-1} (the theoretical curves are according to the Bohart and Adams model); modified by autohydrolysis at 240 °C for 0 min.

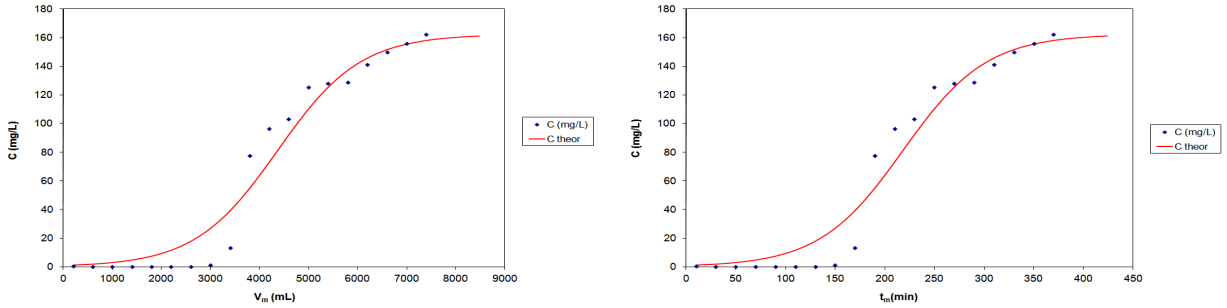

Fig. 6 Column experimental data and theoretical curves of MB adsorption on modified spruce; the effluent concentration is presented vs. (a) the effluent volume and (b) the adsorption time; x = 15 cm, C_i = 160 mg·L^{-1}, Q = 20 mL·min^{-1} (the theoretical curves are according to the Bohart and Adams model); modified by autohydrolysis at 240 °C for 30 min.

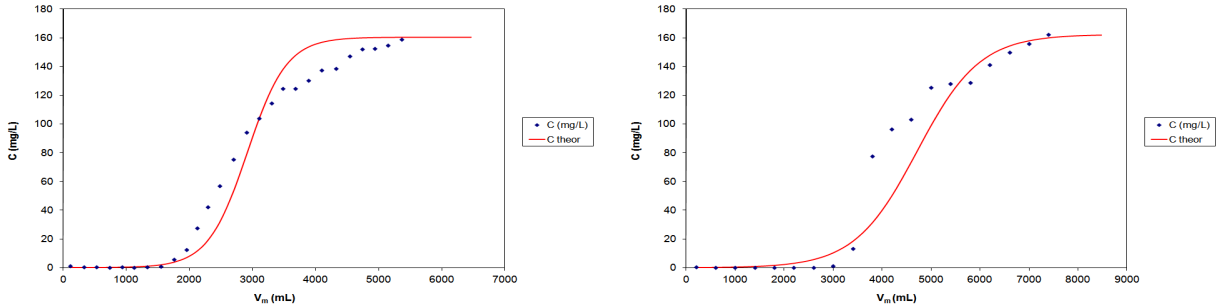

Fig. 7 Column experimental data and theoretical curves of MB adsorption on modified spruce; the effluent concentration is presented vs. (a) the effluent volume and (b) the adsorption time; x = 15 cm, C_i = 160 mg·L^{-1}, Q = 20 mL·min^{-1} (the theoretical curves are according to the Bohart and Adams model); modified by autohydrolysis at 160 °C for 50 min.

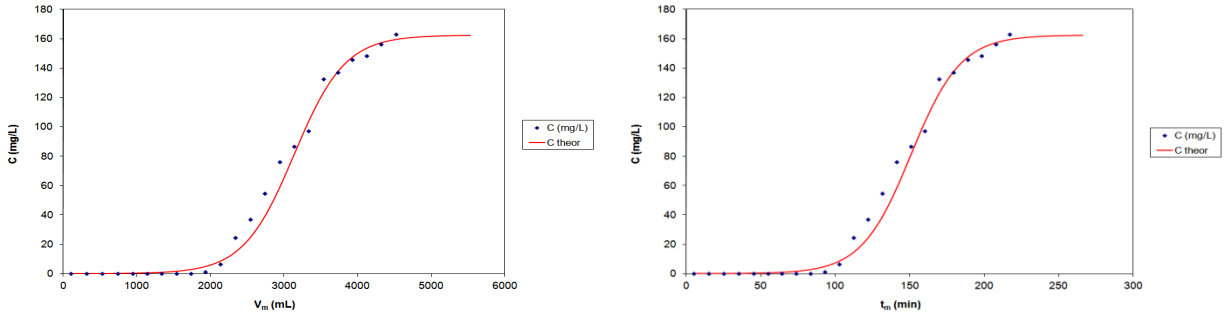

Fig. 8 Column experimental data and theoretical curves of MB adsorption on modified spruce; the effluent concentration is presented vs. (a) the effluent volume and (b) the adsorption time; x = 15 cm, C_i = 160 mg·L^{-1}, Q = 20 mL·min^{-1} (the theoretical curves are according to the Bohart and Adams model); modified by autohydrolysis at 180 °C for 10 min.

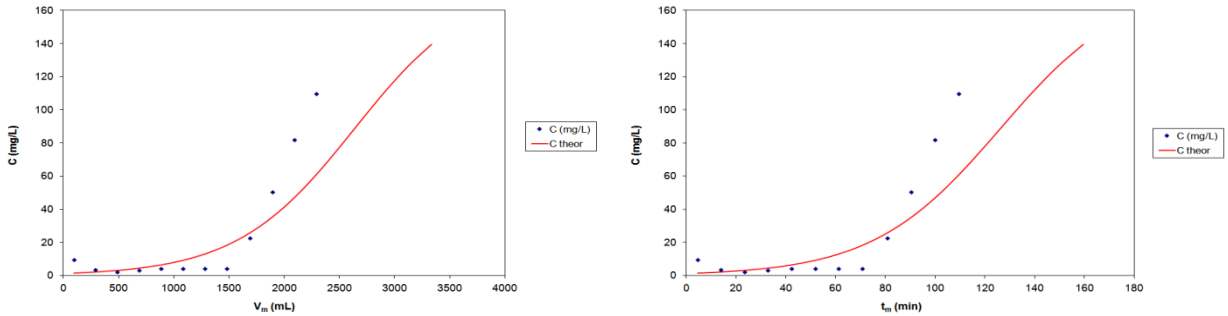

Fig. 9 Column experimental data and theoretical curves of MB adsorption on pine; the effluent concentration is presented vs. (a) the effluent volume and (b) the adsorption time; x = 15 cm, C_i = 160 mg·L^{-1}, Q = 20 mL·min^{-1} (the theoretical curves are according to the Bohart and Adams model).

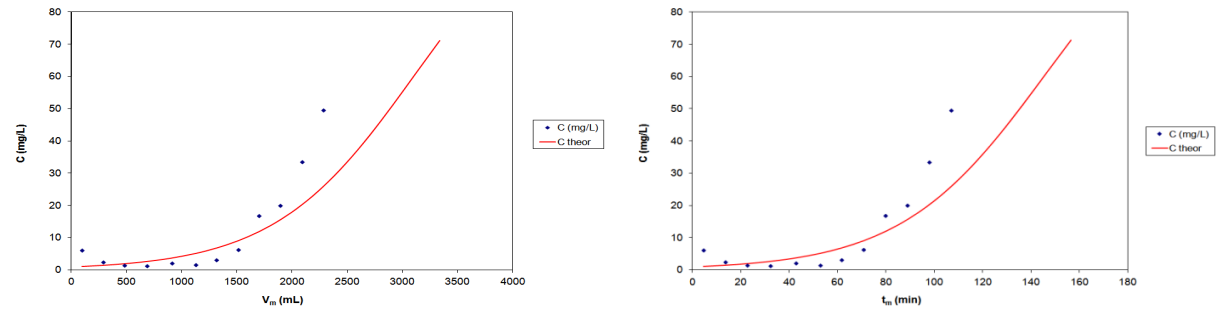

Fig. 10 Column experimental data and theoretical curves of MB adsorption on pine; the effluent concentration is presented vs. (a) the effluent volume and (b) the adsorption time; x = 25 cm, C_i = 160 mg·L^{-1}, Q = 20 mL·min^{-1} (the theoretical curves are according to the Bohart and Adams model).

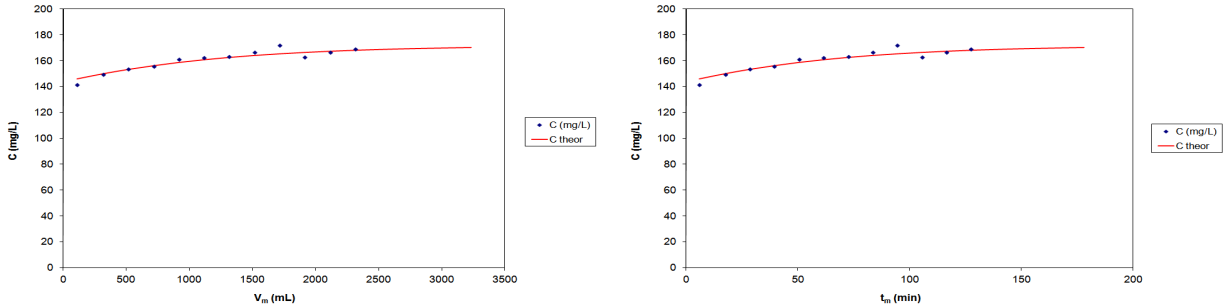

Fig. 11 Column experimental data and theoretical curves of MB adsorption on wheat straw; the effluent concentration is presented vs. (a) the effluent volume and (b) the adsorption time; x = 15 cm, C_i = 160 mg·L^{-1}, Q = 20 mL·min^{-1} (the theoretical curves are according to the Bohart and Adams model).

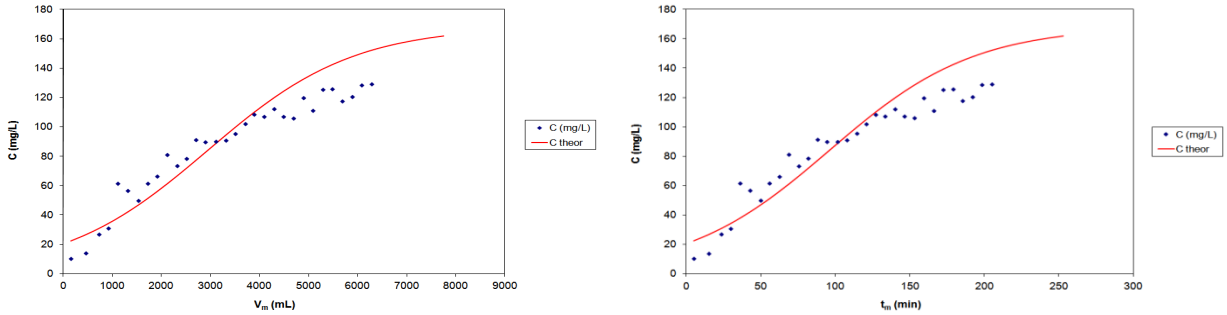

Fig. 12 Column experimental data and theoretical curves of MB adsorption on wheat straw; the effluent concentration is presented vs. (a) the effluent volume and (b) the adsorption time; x = 25 cm, C_i = 160 mg·L^{-1}, Q = 40 mL·min^{-1} (the theoretical curves are according to the Bohart and Adams model).

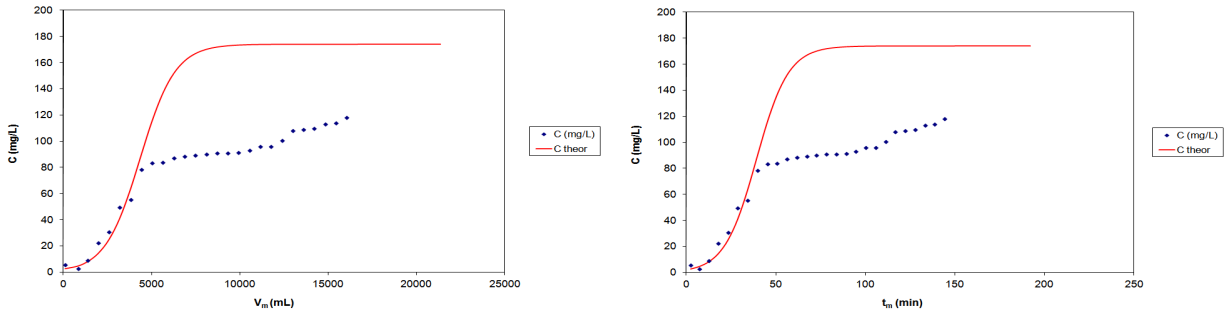

Fig. 13 Column experimental data and theoretical curves of MB adsorption on wheat straw; the effluent concentration is presented vs. (a) the effluent volume and (b) the adsorption time; x = 15 cm, C_i = 160 mg·L^{-1}, Q = 40 mL·min^{-1} (the theoretical curves are according to the Bohart and Adams model).

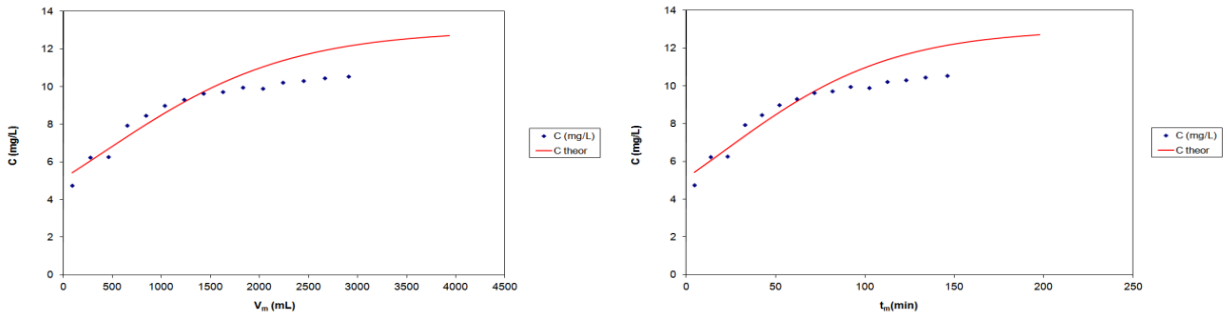

Fig. 14 Column experimental data and theoretical curves of MB adsorption on barley straw; the effluent concentration is presented vs. (a) the effluent volume and (b) the adsorption time; x = 15 cm, C_i = 160 mg·L^{-1}, Q = 20 mL·min^{-1} (the theoretical curves are according to the Bohart and Adams model).

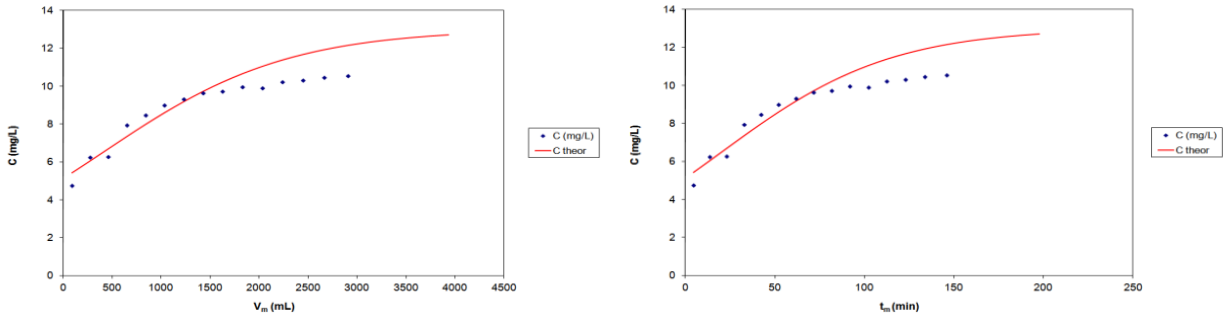

Fig. 15 Column experimental data and theoretical curves of MB adsorption on barley straw; the effluent concentration is presented vs. (a) the effluent volume and (b) the adsorption time; x = 15 cm, C_i = 160 mg·L^{-1}, Q = 20 mL·min^{-1} (the theoretical curves are according to the Bohart and Adams model).

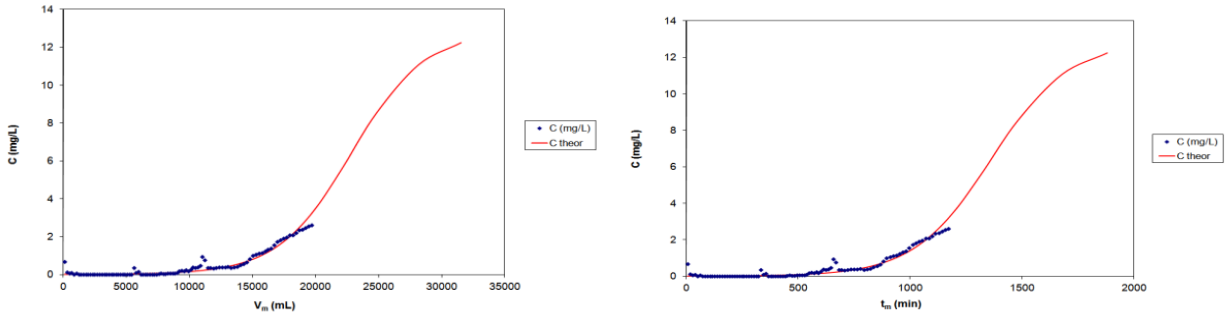

Fig. 16 Column experimental data and theoretical curves of MB adsorption on barley straw; the effluent concentration is presented vs. (a) the effluent volume and (b) the adsorption time; x = 25 cm, C_i = 160 mg·L^{-1}, Q = 20 mL·min^{-1} (the theoretical curves are according to the Bohart and Adams model).

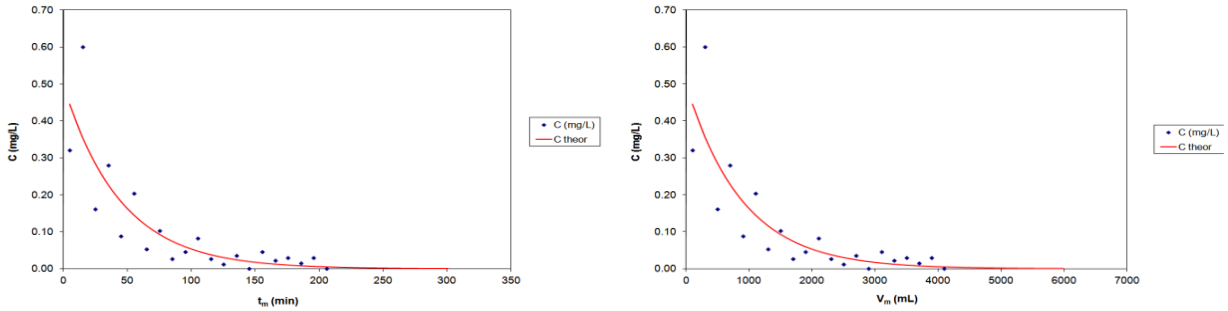

Fig. 17 Desorption of adsorbed at fixed-bed column system. Column experimental data and theoretical curves of MB adsorption on chickpea straw; the effluent concentration is presented vs. (a) the effluent volume and (b) the adsorption time; x = 15 cm, C_i = 160 mg·L^{-1}, Q = 20 mL·min^{-1} (the theoretical curves are according to the Bohart and Adams model).

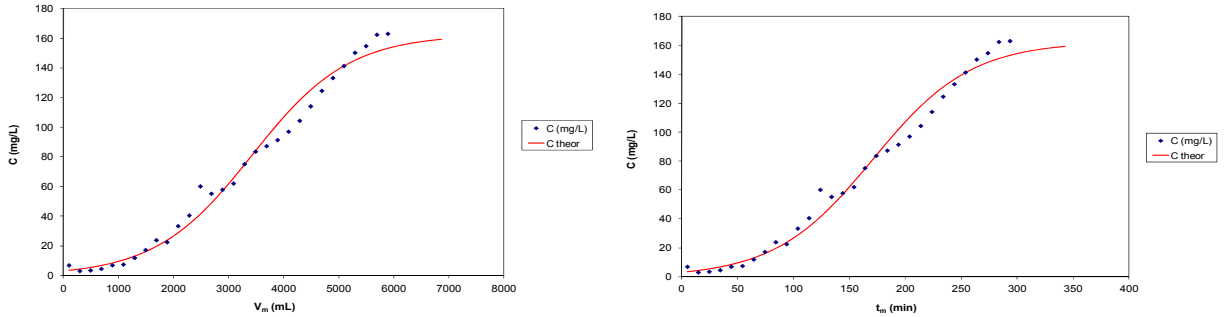

Fig. 18 Column experimental data and theoretical curves of MB adsorption on chickpea straw; the effluent concentration is presented vs. (a) the effluent volume and (b) the adsorption time; x = 15 cm, C_i = 160 mg·L^{-1}, Q = 20 mL·min^{-1} (the theoretical curves are according to the Bohart and Adams model).

concentration in the feed was 165 mg·L^{-1}. The adsorption capacity N was higher at lower flow rate values.

This could be explained by the fact that at lower flow rate, the residence of the adsorbate was longer and hence the adsorbent got more time to bind with the dye efficiently. In other words if the residence time of the solution in the column is not large enough for the adsorption equilibrium to be reached at the given flow rate, the dye solution leaves the column before the equilibrium occurs. It was observed that the adsorbent got saturated easily at higher flow rates. The MB uptake decreased with increase in flow rate. A decrease in flow rate increased the breakthrough time. The breakthrough curve was saturated earlier at higher flow rates because the front of the adsorption zone quickly reached the top of the column. In contrast, lower flow rate and longer contact time, resulted in a shallow adsorption zone. In order to find the effect of bed height on the breakthrough curve, the adsorbate MB solution (initial MB concentration 165 mg·L^{-1}, pH 8) was passed through the adsorption column at a flow rate 70 mL·min^{-1} by varying the bed height. The results showed that the shape and gradient of the breakthrough curve was slightly different from the variation in the bed depth. The concentration of MB in the effluent rapidly increased after the breakthrough point. The lower bed depth (15 cm) gets saturated earlier than the higher bed depth (25 cm).

4. Desorption Results

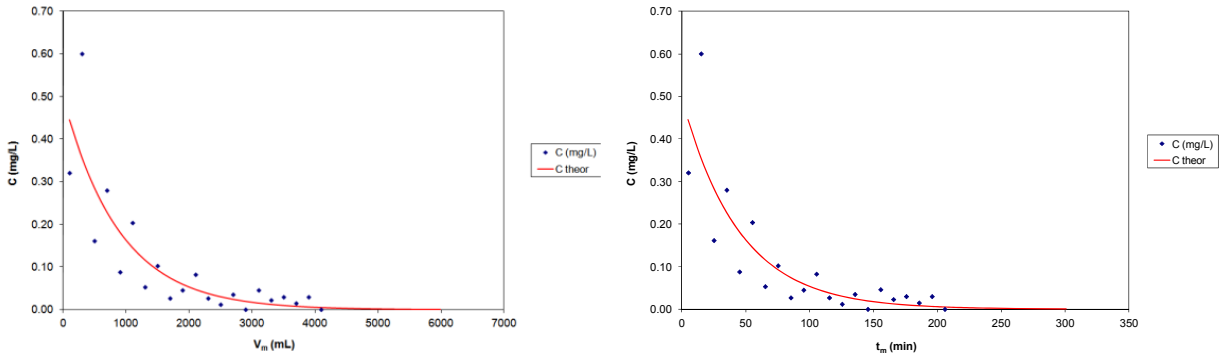

Fig. 19 Column experimental data and theoretical curves of MB desorption from chickpeas straw; the effluent concentration is presented vs. (a) the effluent volume and (b) the desorption time; x = 15 cm, Q = 20 mL·min^{-1} (the theoretical curves are according to the Bohart and Adams model).

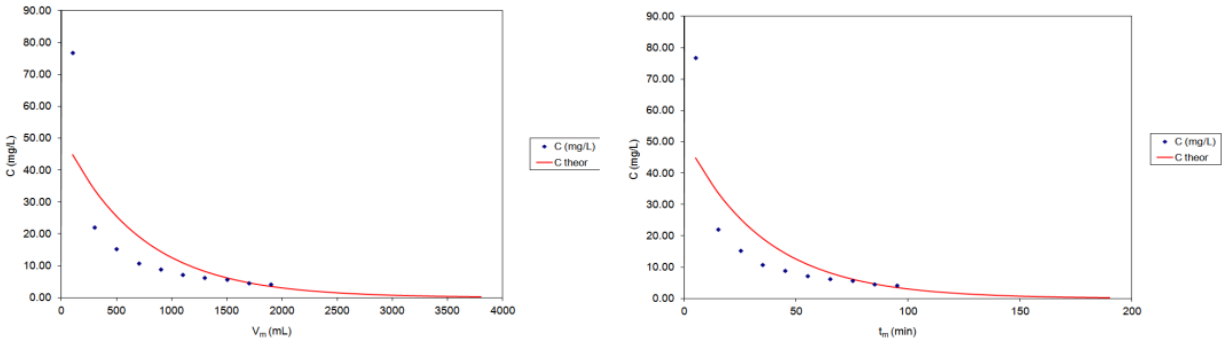

Fig. 20 Column experimental data and theoretical curves of MB desorption on wheat straw; the effluent concentration is presented vs. (a) the effluent volume and (b) the desorption time; x = 15 cm, Q = 20 mL·min^{-1} (the theoretical curves are according to the Bohart and Adams model).

References

[1] Lee, J. M., Shi, J., Venditti, R. A., and Jameel, H. 2009. "Autohydrolysis Pretreatment of Coastal Bermuda Grass for Increased Enzyme Hydrolysis." *Biores. Techn.* 100 (24): 6434-41.

[2] Nabarlatz, D., Ebringerová, A., and Montané, D. 2007. "Autohydrolysis of Agricultural By-Products for the Production of Xylo-Oligosaccharides." *Carbohyd. Polym.* 69 (1): 20-8.

[3] Shukla, A., Zhang, Y.-H., Dubey, P., and Margrave, J. L. 2002. "The Role of Straw in the Removal of Unwanted Materials from Water." *J. Hazard. Mater. B* 95: 137-52.

[4] Crini, G. 2006. "Non-conventional Low-Cost Adsorbents for Dye Removal: A Review." *Biores. Technol.* 97 (9): 1061-85.

[5] Gupta, V. K. 2009. "Application of Low-Cost Adsorbents for Dye Removal—A Review." *J. Env. Manag.* 90: 2313-42.

[6] Gupta, V. K., Carrott, P. J. M., and Ribeiro Carrott, Suhas, M. M. L. 2009. "Low-Cost Adsorbents: Growing Approach to Wastewater Treatment—A Review." *Cr. Rev. Env. Sc. Techn.* 39: 783-842.

[7] Demirbas, A. 2009. "Agricultural Based Activated Carbons for the Removal of Dyes from Aqueous Solutions: A Review." *J. Hazard. Mater.* 167: 1-9.

[8] Rafatullaha, M., Sulaiman, O., Hashim, R., and Ahmad, A. 2010. "Adsorption of Methylene Blue on Low-Cost Adsorbents: A Review." *J. Hazard. Mater.* 177: 70-80.

[9] Nigam, P., Armour, G., Banat, I. M., Singh, D., and Marchant, R. 2000. "Physical Removal of Textile Dyes from Effluents and Solid-State Fermentation of Dye-Adsorbed Agricultural Residues." *Biores. Technol.* 72: 219-26.

[10] Batzias, F. A., and Sidiras, D. K. 2004. "Dye Adsorption by Calcium Chloride Treated Beech Sawdust in Batch and Fixed-Bed Systems." *J. Hazard. Mater. B* 114: 167-74.

Journal of Environmental Science and Engineering A 7 (2018) 172-179
doi:10.17265/2162-5298/2018.04.003

Forage Offer and Nutritive Value of *Elaeagnus angustifolia* in North Patagonia, Argentina

Guadalupe Klich[1], Pedro Bondia[2] and Osvaldo Fernandez[2]

1. Escuela de Veterinaria, Universidad Nacional de Rio Negro. Choele Choel 8360, Argentina

2. Departamento de Agronomia, Universidad Nacional del Sur, Bahia Blanca 8000, Argentina

Abstract: The presence and growth cycle of the browse *Elaeagnus angustifolia* (olivillo, Russian olive), naturalized in the Mid Valley, Rio Negro, Argentina, must be considered in the yearly schedule of rangeland management. Field observations showed that cattle prefer the leaves of this species that are included on the reproductive branches which develop as a thyrse inflorescence. In this trial, authors studied the incidence of *E. angustifolia* in the breeding cow's diet as determined by microhistological analysis of cow feces; mapped the distribution patterns in a cattle farm and quantified its abundance in different parcels; estimated the volume of forage produced by this species and determined the nutritive value of the edible parts of the plants. The quality and quantity of the thyrses accessible for cow's browse suggest that *E. angustifolia* must be considered as an important feed input. The results are used to schedule grazing periods in a valley farm divided into plots with different abundances of *E. angustifolia* and a known floristic composition.

Key words: *Elaeagnus angustifolia*, invader, cattle grazing, forage resource.

1. Introduction

Elaeagnus angustifolia L. (olivillo, Russian olive, Bohemia olive, silverberry, oleaster) is a multiple-stemmed deciduous species of Elaeagnus, native to Eurasia. It was introduced to America in the late 19th century and it became invasive in riparian habitats. It has been reported as alien species in North America [1, 2], in New Mexico [3] and in Argentina [4, 5].

Russian olive has naturalized in the Mid Valley region of Rio Negro Province, in the North of Patagonia, Argentina. It was introduced as a garden tree but escaped from cultivation to colonize the river coastal areas. Several ecological strategies [6] helped this species to spread and naturalize over the valleys, as nitrogen fixation, rapid vegetative propagation, production of numerous seeds, buoyancy of fruits, tolerance to different environmental conditions, adaptation of root system architecture to diverse soil conditions and the allometry of the branches adjusted to compete with various neighboring species.

During the diverse stages, from invasion to colonization of the area, the species received wavering evaluation from the rural coastal cattlemen. Livestock producers first ignored *E. angustifolia* due to unawareness; then they considered it a weed because of the inconvenience it caused in the management of cattle in extensively used fields. When weather conditions turned adverse for cattle breeding due to a long and severe drought in the region, cattle owners realized that the Russian olive tree was a forage alternative [7].

Now that the invasive *E. angustifolia* has been recognized as a forage resource, its presence and phenology must be considered in the yearly schedule of rangeland management.

Previous studies showed leaf heteromorphology [8]. Field observations indicated that cattle prefer the leaves of *E. angustifolia* that are included on the reproductive branches which develop as an indeterminate inflorescence called a proliferating thyrse [9].

Corresponding author: Guadalupe Klich, Ph.D., main research field: applied botany.

Knowledge of the diet of grazing animals is important in developing management standards that allow the proper use of rangelands. The utilization of epidermal characteristics to identify plant components in esophageal, ruminal, or fecal samples is a widespread technique used to study diet composition of free-ranging herbivores [10].

The aims of this field/laboratory trial were to find out the incidence of *E. angustifolia* in the breeding cow's diet as determined by microhistological analysis of cow feces; to map the distribution patterns and quantify the abundance of *E. angustifolia* in different parcels; to estimate the volume of forage produced by this species and to determine the nutritive value of the edible parts of the plants. The results are used to schedule browsing periods in a valley farm divided into plots with different abundances of *E. angustifolia* and a known floristic composition [11-13].

2. Material and Methods

2.1 Study Site

The observations and measurements were made in a 560-hectare cattle farm at the northern margin of Río Negro province, Argentina (39º30′ S, 65º30′ W), where *E. angustifolia* has become naturalized [14]. The region is semiarid, subjected to a great daily and seasonal temperature range, average values fluctuate from 6.83 ºC in the coldest month (July) to 23.02 ºC in the hottest month (January); the medium annual precipitation is 303 mm. Annual evapo-transpiration is over 800 mm, with a negative water balance throughout the year [15]. The farm is divided into parcels of different sizes, distributed from the river coast to the plateau/valley ecotone (Fig. 1). The area, the percentage occupied by *E. angustifolia* and the distribution of the populations were defined for each plot using maps and satellite images (Table 1, Fig. 2).

2.2 Cattle Management

The farm has 12 parcels ranging from 7 to 100 ha, divided with traditional or electric fences to rotate animals grazing. Stocking rates are composed by 110 cows with their 2 to 5-month-old calves (80 to 90) in January and with the remaining yet unsold 7 to 9-month-old calves (around 30) in July. It was planned to use the padlocks with Russian olive for grazing during the spring/summer (October to March).

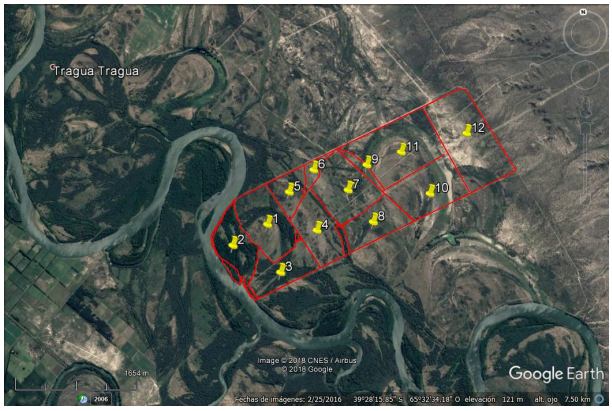

Fig. 1 Cattle farm divided in 12 grazing plots.

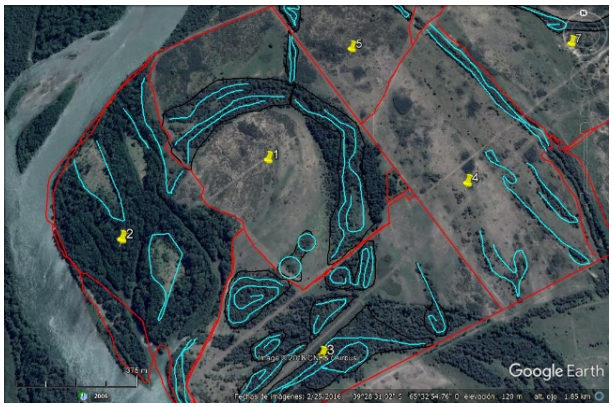

Fig. 2 Detail of some grazing plot showing *E. angustifolia* populations, distributed as invaded rows (light blue) or surfaces (surrounded by a black line).

2.3 Biomass

To estimate the amount of forage that cows may eat from the *E. angustifolia* trees, samples were collected, dried and weighed during all the growing cycle. The edible biomass was calculated considering height the cows can reach to eat the foliage, the thyrse, the number of thyrse per branch, the number of branches per linear meter. The accessibility to the plants was cheeked *in situ*. In open populations the whole surface was recorded. Where the population of *E. angustifolia* follows the course of old river channels authors

considered the dry matter produced on both sides and ignored the production of reproductive branches on the interior of the channels because they were small and of difficult access for the bovines (Fig. 1, detail).

2.4 Diet Microhistological Studies

Plant epidermal characteristics were used to identify components in fecal samples and to study the diet of the cows. Cows' fecal material was collected at the beginning, i.e., 5 days after the entrance of the animal to a plot. For the analysis, 10 slides were made for each of the 20 different cows' feces sampled per date and 40 microscope fields per slide were systematically observed with 100× magnification [10]. The frequency value obtained for each species is converted to density using the table of Fracker y Brischle [16].

Reference slides of leaf, stem and fruit samples of the species present in the area were used for the subsequent identification of epidermal fragments in fecal samples. These slides were prepared with diaphanized material [17], epidermis fragment removed by scraping [18] and according to the method described by Hansen, et al. [19], which used ground material to prepare the samples.

2.5 Feed Analysis

Feed analysis of CP (Crude Protein), ashes (ash), NDF (Neutral Detergent Fiber), ADF (Acid Detergent Fiber), ADL (Acid Detergent Lignin) was made using the sequential method [20], IVDMD (*in Vitro* Dry Matter Digestibility) was determined by Tilley y Terry method [21] in the Animal Nutrition Laboratory, UNS, and are expressed as %. Nutritional analysis (ppm, except chloro as mg/100g) of complete thyrse and separated leaves and fruits in October 2013, January and March 2014, was analyzed with an Atomic Emission Spectrometer (ICP-AES) at LANAQUI laboratory.

2.6 Statistical Analysis

Data were analyzed with ANOVA, and Tukey Test (p-level 0.05).

3. Results and Discussion

Table 1 shows the grazing schedule year-round including all the parcels. The surface of each parcel is shown as well as the portion of the parcel occupied by *E. angustifolia*, expressed in hectares and as percentage of the total surface. The highest records of accessible edible forage were obtained in the middle of the growth cycle, i.e. in January, when the fruits have formed on the thyrses but they are not mature and the seeds are soft and digestible by cows (from February onwards the entire seeds are eliminated in the feces). The edible biomass was calculated considering that cows may eat the thyrses up to 2.50 m in height. Regular weight of thyrse with immature fruits is 11.03 g DM (Dry Matter) and there are usually 20 thyrses per branch. Average 92 reproductive branches were counted in 1 linear meter per 2.5 m height. The maximum dry matter production was estimated as 20.29 kg/m, considering the height the cows can reach (2.5m). The average thyrse weight at the beginning of the growth cycle was 1.80 g DM and when the fruits matured, the mean weight was 8.90 g DM. Biomass production per hectare of the target-plant invaded area and the incidence of its production in the total parcel biomass values, are expressed to compare with *E. angustifolia* consumption evaluated by microhistology as percentage of the total diet of the cows, at the beginning of the grazing period of each plot. The vegetative period of *E. angustifolia* begins in early September, and by the end of the month the first signs of thyrse formation can be detected. The reproductive thyrse elongates during October and the flowers open by the end of the month (Fig. 3a) and continue flowering during November. Small green fruits can be found in December (Fig. 3b). In January the seed inside the fruit is still smooth but it becomes hard in February. The data show that cattle find the thyrse leaves palatable and eat them when moved into a plot (Table 1) specially in the stages from flowering to fruits with smooth seeds (Fig. 3c). Table 2 shows the nutritional and digestibility characteristic of the

Table l Plot number, plot surface (P ha), surface occupied by *E. angustifolia* (E.a. ha), % of the plot area occupied by E.a. (% E.A. inv), edible Maximum expected E.a. biomass offer per plot (t/plot), edible actual expected E.a. Biomass offer per plot (t/plot) and E.a. biomass available per bovine consumption per ha of invaded area. (t/ha inv.) or per plot (t/plot), month of grazing by plot (Month. Gz), consumption at the beginning of the grazing period as determined by microhistology, % of the total diet (% E.a. diet).

Plot No.	ha/plot	ha E.a. /plot	% E.a. inv/plot	E.a. t/plot Max.	E.a. t/plot actual	t E.a./ha inv. max	t E.a./ha plot	Month grazed	% E.a. diet/stage
1	57.0	16.07	28.14	135	33	8.40 b	2.37 f	November	37.26 (flowering)
2	42.0	5.78	13.60	59	43	10.14 d	1.38 e	December	45.69 (small fruit)
3	39.0	11.97	30.72	133	133	11.10 e	3.44 h	January	70.59 (smooth seeds)
4	44.7	6.40	14.31	13	6	20.03 h	2.91 g	February	29.54 (hard seeds)
5	23.2	2.10	9.05	24	6	11.23 f	1.02 d	End October	5.10 (young thyrses)
6	8.0	0.63	7.80	5		7.90 a	0.62 b	gathering paddock	
7	60.1	5.62	9.35	54	5	9.70 c	0.91 c	March	29.00 (hard seeds)
8	40.0	---	---	---		---		April, May	
9	8.0	---	---	---		---		gathering paddock	
10	54.0	---	---	---		---		August	
11	79.0	0.87	0.87	10	1	11.50 g	0.13 a	October	1.80 (small thyrses)
12	110.0	---	---	---		---		June, July	

Different letters in the same column mean significant differences at $p < 0.05$ by Tukey Test.

Table 2 Feed (CP, ashes (ash), NDF, ADF, ADL, IVDMD as %) and nutritional analysis (ppm except chloro as mg/l00g) of complete thyrse and separated leaves and fruits in October 2013, January and March 2014.

Month and material	CP	Ash	NDF	ADF	ADL	IVDMD	K	Ca	Mg	Na	P	S	Cl
Oct. 20l3 initiating thyrse	33.74	7.00	49.43	20.74	4.97	63.84	10,896	4,387	1,615	408	5,022	3,662	229
Jan. 20l4 entire thyrse	15.35	5.11	35.37	22.23	8.53	66.30	2,944	7,817	2,035	951	1,027	1,938	226
Only leaves	22.02	7.41	39.38	22.09	7.27	62.11	3,743	9,904	2,446	1,201	1,149	2,053	300
Only fruits (immature)	8.60	3.44	14.74	9.09	2.82	88.25	3,138	676	436	369	664	590	67
Mar. 2014 entire thyrse	15.27	8.06	37.36	24.67	8.80	62.17	3,851	9,449	1,952	1,371	1,332	2,146	304
Only leaves	20.16	6.94	37.99	21.41	7.08	57.05	8,702	9,040	1,859	1,517	1,418	2,811	341
Only fruits (without seeds)	7.02	3.67	l9.83	12.05	3.81	84.85	6,028	1,369	433	507	582	470	69

different edible parts of *E. angustifolia* in diverse developmental stages.

Traditionally, the coastal cattle farms in Mid Valley of Rio Negro Province have used the spontaneous vegetation as forage resource. Years before this work was started the farm was livestock grazed as an undivided unit. In 2007, it started a long drought period which derived in great regional cattle lost because of the lack of food. Cattle men in riparian areas found out the *E. angustifolia* provided forage and was eaten by cows up to the height the animal could get [7]. Since 2010, the cattle field from where these data were obtained has been divided in small plots and a rotational grazing system has been planned to use efficiently the different forage resources. The Russian olive sites, i.e. those riparian plots and the ones with old river channels, had been used to feed breeding cows during spring and summer, using a schedule of high-density grazing (3 to 5 cow-equivalent/ha) during one month in each plot.

Trees and shrubs, often called browse or topfeed, have long been considered important for the nutrition of grazing animals in other semiarid regions such as Australia, particularly in those areas with a pronounced dry season [22]. They provide the only source of protein and energy during drought. Trees and shrubs do not always have high digestibility, so their energy value may be low. These have been the reasons by

Fig. 3 Thyrses of E. angustifolia.
(a) Flowering stage, (b) immature fruits and (b) cows consume the entire thyrses.

which this study was performed. Authors knew that some parts of the *E. angustifolia* foliage were eaten by cows, but authors needed to obtain animal preference evidence and to evaluate nutritional values.

Previous studies showed leaf heteromorphology [8]. Upper leaves present many xeromorphic characters that enable the trees to maintain their canopy foliage even under the unfavorable conditions (high solar radiation, high temperature, low humidity) during the summer. Lower leaves show many traits of shade leaves and allows the plant to compete for space also in the understory. The author believes that *E. angustifolia* relies on its foliar plasticity, to overcome the environmental gradient between the lower and upper part of a developed tree and even to compete against other species when it grows in places where spatial environment heterogeneity can easily manifest, as in a river valley of a semiarid region.

Field observations showed that cattle eat the leaves of *E. angustifolia* that are included on the reproductive branches which develop as a proliferating thyrse. Lower shade leaves are left intact even when food is scarce, so currently a study is being done to identify and quantify secondary products that make them inedible.

Upper brilliant grey leaves are included in the inflorescence and form long pendular proliferate thyrses. They are consumed by cows from the first stages of inflorescence and fruit formation until early fall, when the fruits are mature, and the seeds are hard and pass through, entire and undigestible, to the feces.

The chemical analysis, the animal voluntary consumption as well as the accessibility of the edible material are factor that must be analyzed together to evaluate the importance of browse plants. Chemical analysis of *E. angustifolia* edible parts has shown important protein content, the highest in blooming thyrses and the lowest in immature fruits, and digestibility over 60%, except in fall leaves. The content of mayor minerals indicates a good input to the cows' diet, specially the Ca and Mg values. The data shown in Table 1 point out that *E. angustifolia*

contributes in a great percentage of the diet and that the animal's voluntary consumes this species thyrses when they enter a new grazing plot. It is important to note that an equal or superior amount of biomass composed of grass and other herbaceous feed is available in each plot when animals enter grazing (unpublished data). The preference for *E. angustifolia* becomes evident specially in the middle of the summer (January) when the fruits are developing and have smooth digestible seeds. The distribution of the species populations in the different plots, the height the cows can reach, their preference for reproductive branches and the parts of the plant included in the cows' bite have been considered when calculating forage offer.

Lamers and Khamzina [23] studied the quality profile and production of foliage from trees grown on degraded croplands of Central Asia and found that the leaves of *E. angustifolia* could be used to supplement protein poor feed rations on dairy cows. The values of feed analysis that they obtained were like authors', considering that they worked on young (4 years old) trees that have not yet begun the reproductive face [6]. They recommend the leaves harvest on the fall based in volume and quality of the leaves. In authors' site, authors have old stablished populations so by fall time the feed quality of the entire thyrse is lesser than during summer time. The fact that the seeds are not digested and pass through to the feces must be considered when evaluating volume and nutritive values.

E. angustifolia can act as a weed and difficult cattle production if the invaded areas are not correctly managed. Division in small plots, short periods (no more than one month) of intense grazing followed by long periods of recovery (until the next year) results in a good exploitation of the forage offer while the grazing and trampling around the mature edible plants maintains the animal access clean from root re-sprouting and other species competence, facilitating the sun light entrance necessary to produce new reproductive edible branches in the next growing cycle.

There are very different opinions on *E. angustifolia* value, but many researches confirm [24, 25] that, once the species is introduced in riparian areas it colonizes replacing the pristine vegetation. Mechanical removal of Russian olive by cutting down or pulling up trees without an herbicide treatment, usually results in a thicker stand of stems, due to its prolific re-sprouting and suckering capacity. Fire has the same effect and sprouting regenerates the population. In cultivated regions of Mid Valley, farmers continue to struggle with this species in the irrigated areas.

According to a recently published review [26], Russian olive should be regarded as a very useful multipurpose tree species. Nevertheless, due to its tendency to spread and colonize bare terrains or areas where it is not desired, a carefully monitoring is necessary to keep this species under control and prevent reduction of diversity. This author mentions also that in the perspective of contemporary climate change, Russian olive could gain more attention from foresters, ecologists and land managers who should develop an integrated management plan for this species.

As mentioned by Lefroy [27], to assess the contribution of browse species to grazing systems it is necessary to consider in turn their forage value to the animals, their economic value to the landholder and their ecological value in the landscape. Authorsadd to the list of characteristics of the species, its forage value, the quality and amount of accessible edible material, without forgetting the natural shelter and shade that it offers to animals in summer time in a semiarid region and the protection of the soil while incorporating nitrogen by actinorryzal symbiosis [6].

4. Conclusions

Mid Valley livestock rangeland must include the foreign specie *E. angustifolia* in the list of spontaneous forage trees present in the riparian zones. A grazing schedule of the cattle farms may improve the quality of feed considering the seasonal forage offer of the naturalized invader. High animal pressure also controls

the species vegetative reproduction and favors accessibility to edible parts of the plant by leaving free the out boundaries of the populations. A proposed management is to use in spring time the grazing-plots located in the riparian zone, which in that season have abundant green herbaceous vegetation of good nutritional quality, while *E. angustifolia* complements the offer. In the scheme of rotations, the paddocks of the area of valley plain should be allocated with population of *E. angustifolia*, to graze in the middle of summer, when the herbaceous vegetation loses water content and nutritional quality due to the heat and drought of these semi-arid zones and the offer of the *olivillo* thyrses, with their immature fruits, it can be the necessary protein contribution for the cows that at that moment are already pregnant and still have their calf with them. Authorspresent this study as an example that using the available rangeland resources more efficiently can substantially contribute to achieving future sustainability goals.

Acknowledgements

This study was funded by Universidad Nacional de Rio Negro and Universidad Nacional del Sur, Argentina.

References

[1] Schaffner, U., Zaquini, L., and Cristofaro M. 2009. "Biological Control of Russian Olive, *Elaeagnus angustifolia*." CABI.

[2] Collette, L. K. D., and Pither, J. 2015. "Modeling the Potential North American Distribution of Russian Olive, an Invader of Riparian Ecosystems." *Plant Ecology* 216 (10): 1-13.

[3] Cox, G. W. 2001. "An Inventory and Analysis of the Alien Plant Flora of New Mexico." *The New Mexico Botanist* 17: 1-8.

[4] Busso, C. A., Bentivegna, D. J., and Fernández, O. A. 2013. "A Review on Invasive Plants in Rangelands of Argentin." *Interciencia* 38 (2): 95-103.

[5] Klich, M. G., Fernandez, O. A., and Weberling, F. 2008. "The Invasive Potential of *Elaeagnus angustifolia* in the Natural Pastures of the Rio Negro Valley, Argentina." In *Proceedings of the XXI International Grassland Congress and the VIII International Rangeland Congress,* volume Ⅱ.

[6] Klich, M. G. 2013. *Olivo de Bohemia*. Saarbrücken: Publicia.

[7] Klich, M. G., and Herrera, S. A. 2018. "Actitudes de los productores ganaderos del Valle Medio de Rio negro, Argentina, durante el proceso de colonización de la arbustiva *Elaeagnus angustifolia* L." In *Malezas e Invasoras de la Argentina Tomo III,* edited by Osvaldo Fernandez, O., Leguizamón, E., Acciaresi, H. and Villamil, C. Bahia Blanca: edi UNS. (in Spanish)

[8] Klich, M. G. 2000. "Leaf Variations in *Elaeagnus angustifolia* Related to Environmental Heterogeneity." *Environmental and Experimental Botany* 44: 171-83.

[9] Weberling, F. 1992. *Morphology of Flowers and Inflorescences*. CUP Archive.

[10] Holechek, J. L., and Gross, B. D. 1982. "Training Needed for Quantifying Simulated Diets from Fragmental Range Plants." *Journal of Range Management* 35: 644-7.

[11] Andrada, A. C., Gil, M. E., Pellegrini, C. N., and. Klich, M. G. 2011. "Spring Floristic Composition in Areas Dominated by *Elaeagnus angustifolia* in the Mid Valley of the Río Negro, Argentina." In *Proceedings of the 2nd World Conference on Biological Invasions and Ecosystem Functioning*, Mar del Plata, Biolief, 88.

[12] Klich, G., Peralta, P., Torres, J. M., Ibañez, R., Neira, D., and Fernández, O. 2018. "Composición del pastizal espontáneo e identificación de las principales especies forrajeras en un campo ganadero del Valle Medio. (Patagonia Norte, Argentina)." *Archivos Latinoamericanos de Producción Animal* 26 (1): 92-3. (in Spanish)

[13] Peralta, P., Torres, J. M., Favere, V., Starnone, N., Ibañez, R., Neira, D., et al. 2018. "Diversidad de grupos taxonómicos en pastizales de campos ganaderos de Patagonia Norte." *Actas VIII Congreso Nacional sobre Manejo de Pastizales Naturales-y IV Congreso del Mercosur sobre Manejo de Pastizales Naturales,* La Rioja. (in Spanish)

[14] Klich, M. G., Bondia, P. M., and Fernandez, O. A. 2018. "*Elaeagnus angustifolia* L." In *Malezas e Invasoras de la Argentina Tomo III,* edited by Fernandez, O., Leguizamón, E., Acciaresi, H. and Villamil, C. Bahia Blanca: edi UNS. (in Spanish)

[15] INTA. 2000. *Resumen de Registros Metereologicos de la Provincia de Río Negro*. Boletín EEA INTA. (in Spanish)

[16] Fracker, S. B., and Brischle, J. A. 1944. "Measuring the Local Distribution of Ribes." *Ecology* 25: 283-303.

[17] Dizeo de Strittmatter, C. G. 1973. "Nueva técnica de diafanización." *Boletín de la Sociedad Argentina de Botánica.* XV (1): 126-9. (in Spanish)

[18] Metcalfe, C. R. 1960. *Anatomy of the Monocotyledons. Volume I. Gramineae*. Oxford: Clarendon. Press.

[19] Hansen, R. M., Foppe, T. M., Gilbert, R. C., Clark, R. C., and Reynolds, H. W. 1977. *The Microhistological Analysis of Feces as an Estimator of Herbivor Dietary. Composition.* Colorado State University: Fort Collins.

[20] Van Soest, P. J., Robertson, J. B., and Lewis, B. A. 1991. "Methods for Dietary Fiber, Neutral Detergent Fiber, and Nonstarch Polysaccharides in Relation to Animal Nutrition." *Journal of Dairy Science* 74 (10): 3583-97.

[21] Tilley, J. M. A., and Terry, R. A. 1963. "A Two-Stage Technique for the *in Vitro* Digestion of Forage Crops." *Grass and Forage Science* 18 (2): 104-11.

[22] Corbet, H. A. 1951. *Fodder Trees; Suggestions for Their Wider Use.* Perth: Imperial Printing Company.

[23] Lamers, J. P. A., and. Khamzina, A. 2010. "Seasonal Quality Profile and Production of Foliage from Trees Grown on Degraded Cropland in arid Uzbekistan, Central Asia." *Journal of Animal Physiology and Animal Nutrition* 94: 77-85.

[24] Katz, G. L., and Shafroth P. B. 2003. "Biology, Ecology and Management of *Elaeagnus angustifolia* L. (Russian Olive) in Western North America." *Wetlands* 23 (4): 763-77.

[25] Tuttle, G. 2017. "Impacts and Management of the Invasive Russian Olive (Elaeagnus angustifolia L.) in a Heterogenous Riparian Ecosystem." PhD thesis, Colorado State University.

[26] Enescu, C. M. 2018. "Russian Olive (*Elaeagnus angustifolia* L.): A Multipurpose Species with an Important Role in Land Reclamation." *Current Trends in Natural Sciences* 7 (13): 54-60.

[27] Lefroy, P. R., Dann, J. H., Wildin, R. N., Wesley-Smith and Mcgowan, A. A. 1992. "Trees and Shrubs as Sources of Fodder in Australia." *Agroforestry Systems* 20 (1-2): 117-39.

Journal of Environmental Science and Engineering A 7 (2018) 180-188
doi:10.17265/2162-5298/2018.04.004

Influence of Percolation Patterns and Soil Copper Concentration on Copper Uptake, and Growth and Yield with Copper-Polluted Stratified Paddy Fields

Jinhun Fan [1], Choichi Sasaki[2], Chihiro Kato[2], Nobuhiko Matsuyama[2], Takeyuki Annaka[3], Akira Endo[2] and Songtao Li[1]

1. The United Graduate School of Agricultural Sciences, Iwate University, Morioka 020-8550, Japan

2. Faculty of Agriculture and Life Science, Hirosaki University, Hirosaki 036-8561, Japan

3. Faculty of Agriculture, Yamagata University, Tsuruoka 997-8555, Japan

Abstract: Copper (Cu) was designated as a specific substance in the Agricultural Land Soil Pollution Prevention Act in Japan. It has been known that high Cu concentrations in soil layers reduce rice crop production and thus agricultural practices such as soil dressing have been applied to minimize the damages to crops by copper pollution. In this study, authors investigated the effects of percolation patterns of the under-plowsole and subsoil on growth and yield, and copper uptake of paddy rice. Six stratified paddy field models were constructed to conduct the growth tests under the condition in which the percolation patterns of the under-plowsole and subsoil were in an open and closed system. These models have a plow layer (10 cm thickness) and upper-plowsole (2.5 cm thickness) made with 12.5 cm-thickness of non-polluted soil dressing (3.7 mgCu·kg^{-1}) and an underlying 15 cm-thickness of polluted under-plowsole (7.5 cm thickness) and subsoil whose Cu concentration was higher or lower than Japanese safety standard (approximately 100 mgCu·kg^{-1}, 150 mgCu·kg^{-1} and 500 mgCu·kg^{-1}, respectively). During the tests, a constant water-ponding system was adopted, and mid-summer drainage was not done. As a result, Cu concentrations of the rice grains were 5% significantly higher in the open system percolation models regardless of the original amount of Cu in the under-plowsole and subsoil. On the other hand, authors did not recognize any significant differences in growth and yield of rice plants among the models. Authors concluded that the Cu concentrations in rice plants are affected by percolation patterns of polluted plowsole and subsoil even though they are covered with non-polluted soil dressing layers.

Key words: Copper, rice plant, percolation patterns, soil dressing.

1. Introduction

Soil contamination by heavy metals is a threat to our health and crop production. In Japan, experiences of serious pollution, such as Itai itai disease caused by cadmium (Cd), caused the waking of the laws which were to prevent heavy metal pollution in 1970's. Cadmium and copper (Cu) are representative of specific substances for regulation [1].

It has been reported that an excess of Cu in soil results in poor growth of rice plants and the upper limit of Cu in soil is specified as 125 mg·kg^{-1} [2, 3]. In Japan, it is recognized that the history of pollution problems started from Ashio copper mine mineral pollution along Watarase River in 1890s. In the 20th century, Japan experienced severe agricultural land contamination caused by the use of mine waste water for agriculture. It took a long time and made much sacrifice to specify the substances which caused the contamination.

For Cd and Cu contamination in agricultural lands, mixing tillage and soil dressing have mainly been conducted [1, 4]. The adoption of a ponding water condition during growing period has also been recommended in order to minimize Cd ad Cu uptake since solubility of these substances decreases under a

Corresponding author: Choichi Sasaki, Ph.D., research field: agricultural land engineering.

reducing condition [5, 6]. In apple orchards in Japan, Bordeaux mixture, a mixture of copper sulphate and calcium carbonate, has been used for long as a pesticide. It is reported that Cu concentrations in the soil of some apple orchards are 4 to 5 times higher than the Japanese standard of Cu concentration (125 mgCu·kg^{-1}) [7, 8].

Nowadays, the number of farmers who quit apple farming has been increasing due to a lack of successors, and some of apple orchards are now used for different purposes. Parts of the apple orchards in lowlands were once converted from paddy fields and they are now restored as paddy fields again [9]. The impact on the adjacent paddy fields of the use of Cu-containing agricultural chemicals in apple orchards should be investigated.

Paul, et al. [10, 11] and Sasaki, et al. [12, 13] clarified that in Cd contaminated paddy fields the percolation patterns of the contaminated plowsole and subsoil would affect Cd concentrations in brown rice significantly even if they had soil dressing layers. Paul, et al. [11] also mentioned that the amount of Cu uptake by the rice plants would be affected by percolation patterns, although they had used low-level Cu-containing soil (12.2 mgCu·kg^{-1}) in their experience. Since solubility of Cu increases under the oxidation condition and decreases under the reduction condition (the same reactions happen in Cd [14]), percolation pattern of stratified paddy fields may have a significant impact on Cu uptake and growth and yields of rice plants in Cu contaminated paddy fields.

It has been pointed out that Cu contaminated soil reduces the number of panicles and the ratio of ripening of rice plants, and causes Cu accumulation in their roots [15, 16]. Shibuya [16] also reported that the yield of brown rice decreased by around 10% with Cu contaminated subsoil (over 200 mgCu·kg^{-1}) and 15 cm thickness of soil dressing. Those studies, however, did not consider the percolation patterns of the subsoil in stratified paddy fields. Fan, et al. [9] conducted the growth experiments of rice plants with stratified paddy filed models of two different Cu concentrations, 70 mgCu·kg^{-1} and 250 mgCu·kg^{-1}; Japanese safety standard is 125 mgCu·kg^{-1}. They reported that Cu concentrations in the brown rice of the open type percolation models were significantly higher by 5% than those of the closed type percolation models. In the models with a concentration of Cu (241 mg·kg^{-1}), the Cu concentration in stems and leaves and roots showed significantly different values between the percolation patterns.

In this study, in order to clarify the effects of percolation patterns on Cu uptake and growth and yield of rice plants in Cu contaminated paddy fields, adding to Fan, et al. [9], authors conducted the growth experiments with the Cu-contaminated stratified paddy field models of 100 mgCu·kg^{-1}, 150 mgCu·kg^{-1}, and 500 mgCu·kg^{-1}, one is below Japanese safety standard and the other two are above the standard.

2. Material and Methods

2.1 Soil Samples

In this study, authors used soils stratified in the same way as Fan, et al. [9]. Table 1 shows physical and chemical properties of the soils (modified Fan, et al. [9]). Non-contaminated soil (Clay loam; International Union of Soil Science) was collected from the plow layer of the paddy field in Kanagi farm of Hirosaki University, Aomori, Japan (hereafter authors call "Kanagi Soil"). Cu contaminated soils were prepared for this study by adding copper chloride (Ⅱ) hydrate ($CuCl_2 \cdot 2H_2O$) to the soil (Loam) which had been sampled from plow layer of the paddy field in Bunkyo campus of Hirosaki University, Aomori, Japan (hereafter "Bunkyo soil") and they were mixed well.

Additionally, 0.1 M HCl extracted-copper concentrations in Kanagi soil and Bunkyo soil were originally 3.7 mgCu·kg^{-1} and 10.5 mgCu·kg^{-1}, respectively, and by using them, three levels of Cu contained soils, 100 mgCukg^{-1}, 150 mgCu·kg^{-1} and 500 mgCu kg^{-1}, were made (hereafter "Cu mixed

Table 1 Physical and chemical properties of the soil (modified by Fan, et al. [9]).

	Density	Soil texture	MgO	CaO	K_2O	Cu	T-C	T-N	C/N	OM
	($g \cdot cm^{-3}$)				($mg \cdot kg^{-1}$)		(%)	(%)		(%)
Kanagi Soil	2.58	L	229	531	306	3.70	2.74	0.18	15.40	4.70
Bunkyou Soil	2.61	CL	219	1,848	373	10.50	3.84	0.26	14.50	6.60
Gravel	2.68	-	-	-	-	0.80	0.04	0.01	4.00	0.10

Note: Tukey-Kramer test was performed at 5% level; letter indicates significant difference.

soils"). Cu concentration in the gravel used in the models was 0.8 $mgCu \cdot kg^{-1}$. Cu mixed soils contain 20 to 100 times higher than the average Cu concentration in soils in non-contaminate paddy fields in Japan (approximately 5 $mgCu \cdot kg^{-1}$) [1]. TC (Total Carbon) and TN (Total Nitrogen) in the soils were measured by using CN analyzer (Elementar). The organic matter contents, which were calculated with TC percentage, of Kanagi soil and Bunkyo soil were 7.4% and 6.6%, respectively. The gravel was packed as the lower layer of the experimental models since they were designed after the fashion of paddy fields near a river.

2.2 Experimental Design

According to the report by Sasaki, et al. [12], two types of stratified paddy field models were used for the experiment: the open-system percolation model and the closed-system percolation model. Each stratified paddy field model was constructed in an iron box (30 cm × 50 cm × 70 cm) filled with three layers of soil. The first layer (plow layer) was 10 cm depth with non-polluted Kanagi Soil (soil dressing, dry density in puddling condition was 1.04 $g \cdot cm^{-3}$). The second layer (plowsole) was 2.5 cm depth with soil dressing and 7.5 cm depth with polluted soil (Cd mixed soil, dry density at the depth from 10 cm to 12.5 cm and from 12.5 cm to 20 cm were 1.23 $g \cdot cm^{-3}$ and 0.75-0.95 $g \cdot cm^{-3}$, respectively). The third layer (subsoil) was 7.5 cm depth with polluted soil and 35 cm depth with non-polluted gravel (dry density at the depth from 20 cm to 27.5 cm and from 27.5 cm to 55 cm were 0.75-0.95 $g \cdot cm^{-3}$ and 1.40 $g \cdot cm^{-3}$, respectively, those layers were formed by compaction). The authors defined O-100 and C-100 as the Cu concentration of 100 $mg \cdot kg^{-1}$ in the each stratified paddy field model ("O" and "C" stand for the open-system and the closed-system percolation, respectively). Similarly, O-150 and C-150 were defined as the Cu concentration of 150 $mg \cdot kg^{-1}$, O-500 and C-500 were defined as the Cu concentration of 500 $mg \cdot kg^{-1}$, respectively. The percolation patterns were determined by Sasaki, et al. [17]. The ground water levels of the open-system and the closed-system percolation models were controlled at 57.5 cm and 12.5-20 cm depth, respectively. In the closed-system percolation models, the holes on the side of the iron box were blocked in order to prevent the penetration of the atmosphere. On the other hand, in the open-system percolation models, the holes on the side of the iron box were open in the lower part of the plowsole and the upper part of the subsoil in order to aerate those layers. After the two types of models were prepared, fifteen paddy seedlings (plant length and leaf stage were about 15 cm and about 5.0 leaves, respectively) named "*Oryza sativa* L., Tsugaru Roman" were transplanted. The paddy seedlings were transplanted by 10 cm intervals. The rate of fertilizer application was of the standardized value (2 g of N, 2 g of P_2O_5 and 2 g of K_2O). The topdressing was not done during the growing period. While the cultivation period, the water ponding condition was constantly adopted and the mid-summer drainage was not done. Transplanting of the paddy seedlings and harvesting were conducted at the end of May and at the middle of September, respectively. The experiment using the stratified paddy field models was conducted in a greenhouse on the university campus.

2.3 Measuring Method

The examination of rice plants was done by the standard method of Iwate Agricultural Experimental Station [18]; authors examined such details as plant length, leafage, the number of stems and panicles, the weight of straw, the number of brown rice and the weight of brown rice. The quantitative analysis of Cu concentrations in foliage, roots (depth of 0-10 cm), brown rice and soils extracted by HCl solution was measured with atomic absorption spectroscopy [19]. Other measurements were also conducted in standard methods used in Japan. The ORP (Oxidation-Reduction Potential) meter (Central Kagaku Co., Ltd., UC-203) was used for measuring oxidation-reduction potential (Eh). ORP sensors were set at each soil layer.

3. Results and Discussion

3.1 Oxidation-Reduction Potential (Eh)

In this study, oxidation and reduction condition was defined as Eh > 300 mV and Eh < 300 mV, respectively, based on Yamane [20]. The temporal changes of Eh are shown in Figs. 1 to 4. The plow layer of O-100 and O-500 in the open system percolation pattern became the reduction layer (under -100 mV), while the plowsole and the subsoil became an oxidation layer (over 300 mV). On the other hand, Eh values measured at each depth of O-100 and O-500 in the closed system percolation patterns gradually decreased after transplanting and Eh of all depths became a reduction layer as under 0 mV. Because these Eh data approximated O-100 and C-100, the results of O-150 and C-150 are omitted here.

In this result, the contaminated soil layer became an oxidation layer in three models of O-100 to O-500. However, in the model of C-100 to C-500, the same layer became a reduction layer. It is pointed out that the uptake of Cu in rice is influenced by oxidation-reduction environment [5]. However, the Eh value of the oxidation layer represented in Fig. 3 was lower than that in Fig. 1, and it seemed that the Eh measured below the plowsole had a weak reduction condition represented in Fig. 4. This is thought to be due to the fact that the packing dry density of the soil layer model was somewhat higher and also that the soils used in the experiment were not the same kind. However, details are not clear and the issue needs further examination.

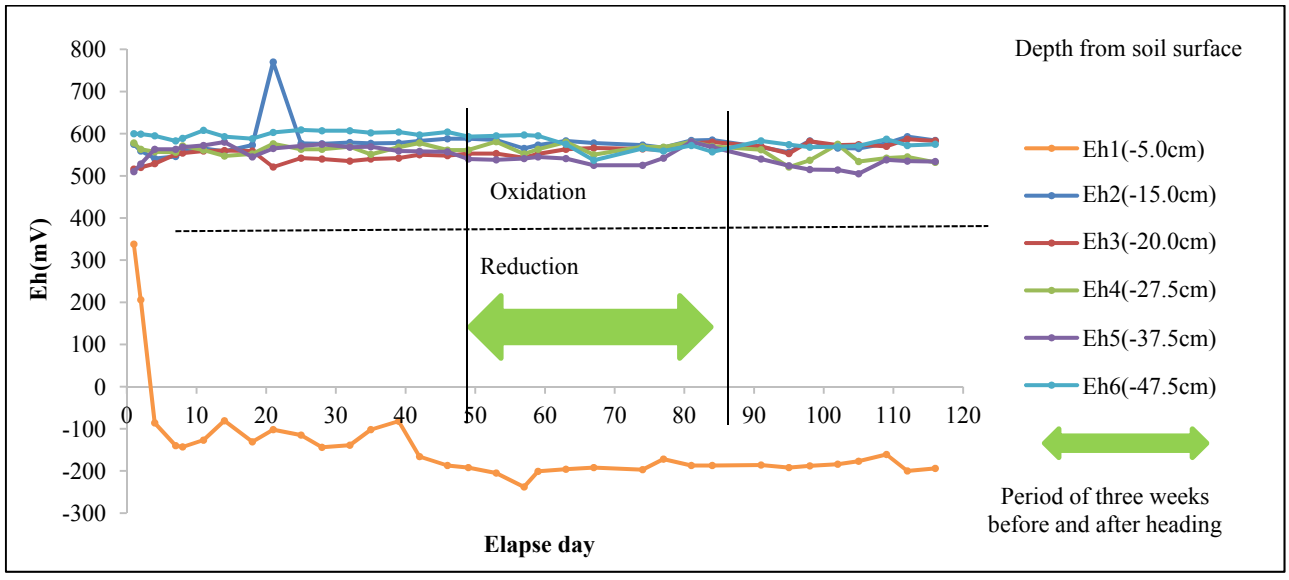

Fig. 1 Temporal changes of Eh in the stratified paddy field model (O-100).

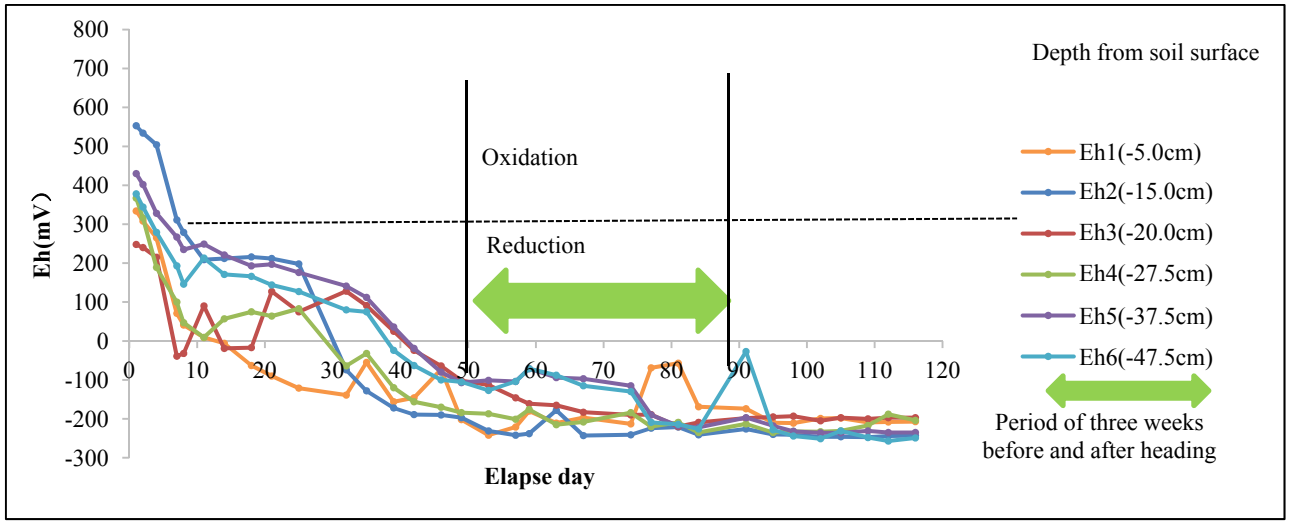

Fig. 2 Temporal changes of Eh in the stratified paddy field model (C-100).

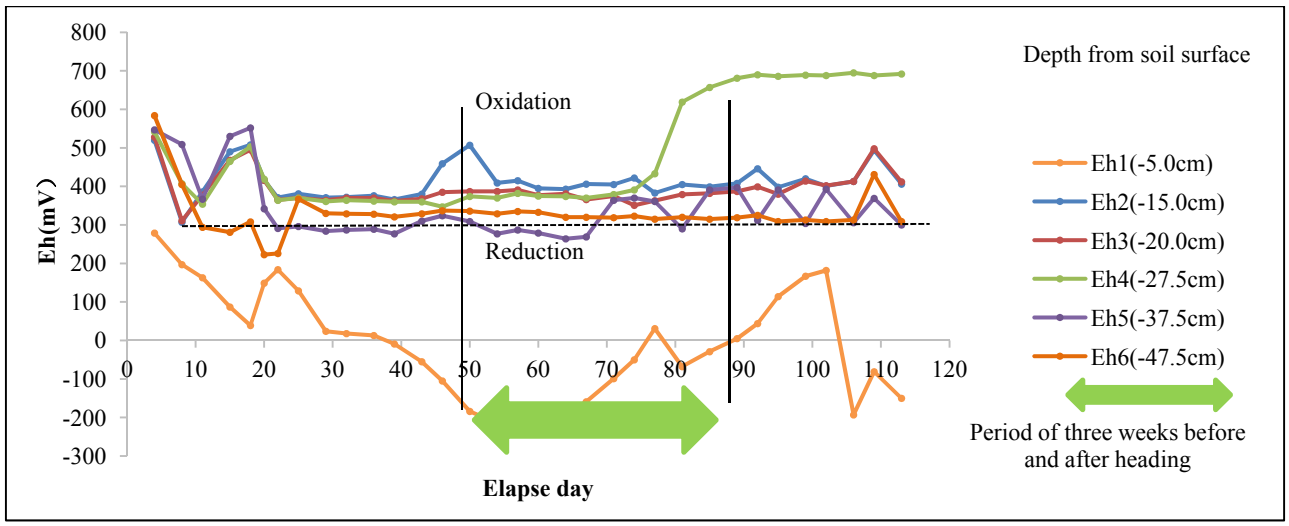

Fig. 3 Temporal changes of Eh in the stratified paddy field model (O-500).

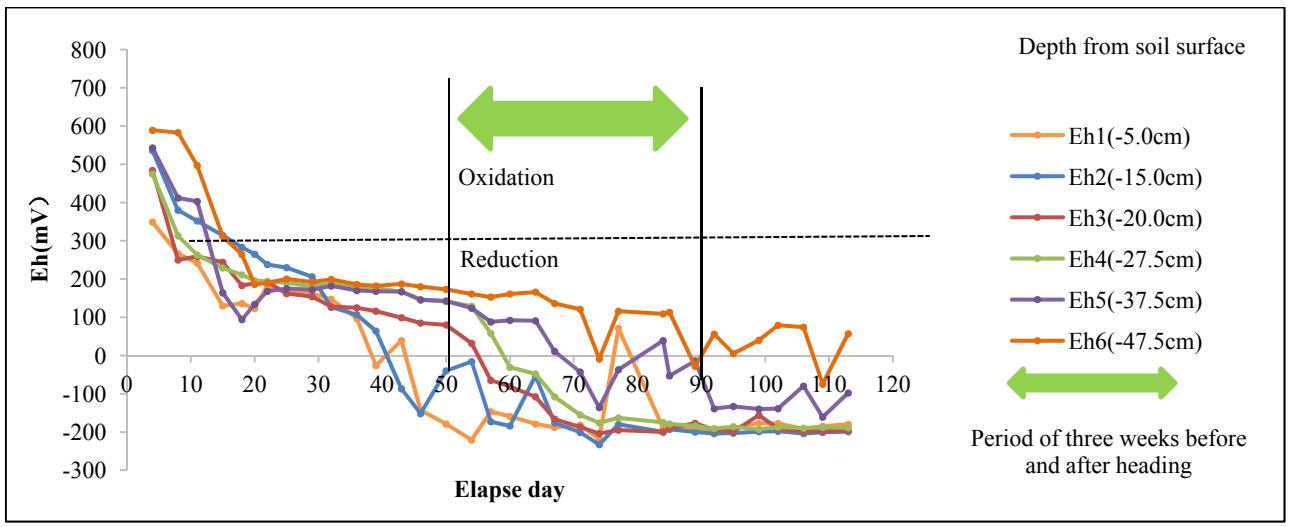

Fig. 4 Temporal changes of Eh in the stratified paddy field model (C-500).

Table 2 The results of Cu concentration in rice plants.

	Rice grains (n = 7)	Roots of plow layer (n = 5)	Stems and leaves (n = 5)
Model	(mg·kg^{-1})	(mg·kg^{-1})	(mg·kg^{-1})
O-100	3.9 ± 0.4^{a}	16.4 ± 1.3^{a}	1.2 ± 0.4^{a}
C-100	3.3 ± 0.1^{bd}	14.9 ± 0.7^{a}	1.2 ± 0.1^{a}
O-150	4.7 ± 0.7^{c}	19.8 ± 1.6^{b}	1.8 ± 0.4^{bc}
C-150	3.4 ± 0.3^{ab}	20.2 ± 0.9^{b}	1.1 ± 0.4^{a}
O-500	3.7 ± 0.2^{ab}	15.3 ± 1.2^{a}	2.1 ± 0.1^{b}
C-500	2.8 ± 0.1^{d}	16.3 ± 0.9^{a}	1.4 ± 0.2^{ac}

Note: Tukey-Kramer test was performed at 5% level; letter indicates significant difference. The numerical value of ± shows standard deviation.

3.2 Copper Concentration in Rice Plants

The results of Cu concentration in rice plants are listed in Table 2.

(1) Rice Grains: Cu concentration in brown rice (n = 7) was ranged from 2.8 to 4.7 mg·kg^{-1}. The tendency of Cu concentrations due to the difference in percolation type was O-100 > C-100, O-150 > C-150 and O-500 > C-500. These were similar to the Cu concentrations indicated by Asami [1]. However, in his study, there was no demarcation in the percolation types. In our study, Cu concentrations in the rice grains of the open system percolation models were significantly higher by 5% than the ones of the closed system percolation models. Paul, et al. [11] reported that the significant difference was observed in Cu concentrations in brown rice due to differences in percolation patterns. In the same study, the Cu concentrations in brown rice ranged from 2.5 to 4.2 mg·kg^{-1}, even though the Cu concentrations were low at about 10 mg·kg^{-1}. Taking these results also into consideration, authors can suggest that the Cu concentrations ranging from 10 to 500 mg·kg^{-1} in the lower layer did not give a significant difference in Cu concentrations in brown rice. From the above results, it was confirmed that the difference in Cu concentrations in brown rice was made due to the difference in percolation types. This was similar to the results of the Cd contaminated soil experiment conducted by Sasaki, et al. [12, 13].

(2) Stems and Leaves: Since the Cu concentrations in the stems and leaves of every percolation model became less than 2 mg·kg^{-1}, statistically significant differences were not observed in the Cu concentrations. However, significant differences were observed in the percolation models of O-150 > C-150 and O-500 > C-500. Although migration of Cu was small, there was a possibility that a significant difference in Cu concentrations might be made in stems and leaves in the contaminated soil of the lower layer in more than 125 mg·kg^{-1}. It is speculated that the differences between low and high Cu concentrations in the soil are causing this difference.

(3) Roots: Cu concentrations in roots (n = 7) ranged from 14.9 to 20.2 mg·kg^{-1}. High Cu concentrations observed in the percolation model of O-500 (15.6 mg·kg^{-1}) were not very different from those observed in the models of O-100 (16.4 mg·kg^{-1}). Any significant differences in Cu concentrations were not observed between different percolation system models. Even if there is no significant difference in the Cu concentrations in roots, however, it is presumed that there is a difference in the migration mechanism to the aerial part.

Cu concentrations in the rice plants were in the order of roots > brown rice > stems and leaves, and the ratio was 12:3:1. This order was similar to that of Shibuya [16] and Paul, et al. [11] who used rice plants, and to those of Li, et al. [21] who used soybeans. It was predicted that these results were due to the transport characteristics of Cu and Cd in the rice plants. The behavior of Cu concentrations in brown rice is presumed to be almost constant even if Cu concentrations in the soil rise in the same way as the

Table 3 Parameters of rice plant growth (n = 8).

Model	Plant length (cm)	Leaf age (leaf)	Weight of dry straw (g·hill^{-1})
O-100	94.3 ± 3.6^{a}	14.0 ± 0.0^{a}	11.6 ± 2.4^{a}
C-100	99.9 ± 2.8^{ab}	14.4 ± 0.5^{b}	13.9 ± 2.8^{a}
O-150	101.6 ± 4.5^{b}	14.0 ± 0.0^{a}	13.0 ± 1.9^{a}
C-150	99.1 ± 2.8^{ab}	14.0 ± 0.0^{a}	13.5 ± 2.4^{a}
O-500	101.0 ± 6.1^{b}	15.0 ± 0.0^{c}	11.8 ± 2.8^{a}
C-500	101.3 ± 2.9^{b}	15.0 ± 0.0^{c}	12.6 ± 2.3^{a}

Note: Tukey-Kramer test was performed at 5% level; letter indicates significant difference. The numerical value of ± shows standard deviation.

Table 4 Parameters of rice plant yield (n = 8).

Model	The weight of one panicle (g)	No. of Panicles (Panicles·hill^{-1})	The percentage of ripening (%)	The number of brown rice per unit hill (grains·hill^{-1})	The 1,000 grain weight of brown rice (g)
O-100	2.2 ± 0.6^{a}	8.5 ± 1.7^{a}	94.0 ± 2.2^{a}	553.3 ± 133.2^{a}	19.2 ± 0.6^{a}
C-100	2.2 ± 0.3^{a}	9.5 ± 2.5^{a}	93.6 ± 2.8^{a}	710.4 ± 170.4^{a}	19.3 ± 0.6^{a}
O-150	2.0 ± 0.2^{a}	8.8 ± 0.7^{a}	93.8 ± 1.4^{a}	642.9 ± 103.9^{a}	18.9 ± 0.3^{a}
C-150	2.2 ± 0.3^{a}	8.9 ± 2.3^{a}	94.3 ± 2.3^{a}	670.4 ± 128.1^{a}	19.6 ± 0.3^{a}
O-500	2.4 ± 0.4^{a}	7.0 ± 1.4^{a}	97.5 ± 0.6^{b}	579.4 ± 99.7^{a}	22.8 ± 0.5^{b}
C-500	2.6 ± 0.2^{a}	7.1 ± 1.7^{a}	97.4 ± 0.7^{b}	621.3 ± 149.5^{a}	23.2 ± 0.8^{b}

Note: Tukey-Kramer test was performed at 5% level; letter indicates significant difference. The numerical value of ± shows standard deviation.

behavior of Zn concentrations reported by Shibuya [16].

3.3 Growth and Yield of Rice Plants

The results of this experiment in for the growth and yield of rice plants are shown in Tables 3 and 4, respectively.

(1) Growth of rice plants: The average plant height (n = 8) of each model was almost equal, and it was between 94.3 to 101.3 cm (Table 3). Leafage of each model was ranged from 14.0 to 15.0, showing little difference between them. Total straw weight was 11.6-13.9 g·hill^{-1}. No significant difference was observed in the plant height, leafage and total straw weight regardless of the percolation patterns. Previous research by Shibuya [16] reported that Cu concentrations in the Cu polluted soil layer had an influence on the growth of rice plants. In this study, however, the influence of the Cu concentrations on the growth of rice plants was not noticeable, which may have resulted from the application of soil dressing. A similar result was obtained by Fan, et al. [9].

(2) Yield of rice plants: The number of panicles per unit hill in each model was between 7.0 and 9.5 hill^{-1} (Table 4). Likewise, weight of one panicle and the number of grains of brown rice per unit hill were between 2.2 and 2.6 g·panicle^{-1} and between 553 and 710 grains·hill^{-1}, respectively. In addition, the percentage of ripening and the 1,000 grain weight of brown rice were between 93.6 and 97.5% and between 18.9 and 23.2 g, respectively. No significant differences were found in any of the items of the models in different percolation types, which also agreed with the results of Fan, et al. [9]. Paul, et al. [10] reported that yield components of the closed-system percolation model were significantly higher than those of the open-system percolation model although their experiment was conducted by using a different soil type for Cd polluted soil layers.

Shibuya [16] reported that Cu concentrations had an influence on the number of panicles and the percentage of ripening. In this study, however, the influence of the Cu concentrations on the growth of rice plants was not remarkable, which may be attributed to the application of soil dressing. Shibuya [16] also reported that the yield of brown rice decreased by about 10% under a Cu concentration condition of higher than 200 mg·kg^{-1} with a 15-cm thick soil dressing. Authors inferred, however, that Cu concentration did not cause a remarkable difference in the yield of rice plants if they were within the range of Cu concentrations adopted in this study and that of Fan, et al. [9].

4. Conclusion

Using six types of Cu-polluted stratified paddy field models, authors conducted an experiment to clarify the effects of percolation patterns in the sub-layer (both plowsole and subsoil) on the Cu concentrations in rice plants and their growth and yield. The models had a 15-cm thick Cu polluted soil layer and a 12.5-cm thick non-polluted soil dressing. For the Cu polluted soil layer, three different Cu concentrations of 100 mg·kg^{-1}, 150 mg·kg^{-1} and 500 mg·kg^{-1} were prepared.

The results of our experiment showed that in the open system percolation models the sub-layers became oxidation layers and in the closed system percolation models the sub-layers became reduction layers. Cu concentrations in the brown rice of the open system percolation models were significantly higher by 5% than those observed in the closed system percolation models. However, there was little significant difference in the growth and yield of rice plants between the percolation patterns.

Under the above conditions, difference in percolation patterns of the stratified paddy field models little affected the growth and yield of rice plants, while it had an influence on Cu concentrations in the rice plants.

Acknowledgement

The authors appreciate the cooperation of Fujita Masayoshi and Takahashi Yuto who cooperated in carrying out this research. In addition, this research was conducted under the support of Grant-in-Aid for Scientific Research (No. 26660188). Authors would like to thank everyone concerned.

References

[1] Asami, T. 2010. *Toxic Metal Concentration in Japan*. Tokyo: Agune Technology Center Ltd..

[2] Yamane, I. Hamada, R., Yoshinaga, N., Asami, T., Matsuda, K., Sakuma, T., et al. 1998. *Soil Science*. Tokyo: Bunneidou.

[3] Tkaishi, M., Oshima: H., and Asano. S. 2015. "Pollution Caused by Ashio Copper Mine and Its Effects on Environment and Human Health." *Journal of International University of Health and Welfare* 20 (2): 59-69.

[4] Akahane, I., Makino, T., Katou H., Nakamura K., Sekiya N., Kamiya T., and Takano H. 2013. "Remediation of Cadmium-Contaminated Arable Soils by Washing with Iron (III) Chloride." *Journal of Japanese Society of Soil Physics* 123: 55-63.

[5] Matsunaka, T. 2014. *Basic Soil Science*. Tokyo: Nobunkyo.

[6] Inahara, M., Ogawa, Y., and Azuma, H. 2007. "Countermeasure by Means of Flooding in Latter Growth Stage to Restrain Cadmium Uptake by Lowland Rice." *Japanese Journal of Soil Science and Plant Nutrition* 78: 149-55.

[7] Inoue, H., Masuda, K., Sakamoto, K., Nukada, M., Umemiya, Y., and Kita, M. 2007. "Copper Accumulation and Chemical Forms in Brdeaux Mixture Spraying Apple Ochard Soil." *Japanese Journal of Soil Science and Plant Nutrition* 78: 81-3.

[8] Aoyama, M. 2009. "Characteristics of the Apple Orchard Soils and the Effects of Compost." In *Science of the Apple,* Open Lecture in Teaching and Research Center for Bio-coexistence, Faculty of Agriculture and Life Science, Hirosaki University, 35-42.

[9] Fan, S., Sasaki, C., Matuyama, N., Annaka, T., Endo, A., Li, S., and Sasaki, K. 2018. "Influence of Percolation Patterns on Copper Uptake, and Growth and Yield with Copper-Polluted Stratified Paddy Fields." *International Journal of Environmental and Rural Engineering* 9 (in press).

[10] Paul, S. K., Sasaki, C., Matsuyama, N., Noda, K., and Mitra, B. K. 2011. "Influence of Percolation Patterns on

Growth and Yield of the Rice Plants and Uptake of Cadmium from Polluted Paddy Fields Using Soil Dressing Models." *Pedologist* 54: 222-9.

[11] Paul, S.K., Sasaki, C., Matsuyama, N., and Kato, K. 2011. "Effect of Percolation Pattern on Yields and Accumulation of Copper and Cadmium in the Rice Plants with Soil Dressing Models." *Environmental Science and Engineering* 5: 1464-73.

[12] Sasaki, K., Sasaki, C., Kato, C., Endo, A., Annaka, T., Moritani, S., and Matsuyama, N. 2016. "Studies on Reducing Cadmium Uptake of Paddy Rice (*Oryza stative* L.) by Both Soil Dressing and Mixing Tillage." *International Journal of Environmental and Rural Engineering* 7: 6-14.

[13] Sasaki, K., Sasaki, C., Kato, C., Annaka, T., and Matsuyama, N. 2016b. "Effects of the Percolation Patterns and the Thickness of Soil Dressing on Reducing Cadmium Uptake and Growth and Yields of Rice Plants (*Oryza stative* L.)." *Journal of Environmental Science and Engineering* A5: 11-20.

[14] Dong, J., Mao, W. H., Zang, G. P., Wu, F. B., and Cai, Y. 2007. "Root Excretion and Plant Tolerance to Cadmium Toxicity—A Review." *Plant, Soil and Environment* 53 (5): 193-200.

[15] Chino, M., and Kitagishi, K. 1966. "Heavy Metal Toxicities in Rice Plants (Part 2): The Toxicities of Copper, Nickel, Cobalt, Zinc and Manganese at Different Stages of the Plant Growth." *Japanese Journal of Soil Science and Plant Nutrition* 37: 372-7.

[16] Shibuya, M. 1979. *Mechanism and Analysis of Soil Pollution*. Tokyo: Sangyo-tosho, 3-15.

[17] Sasaki, C. 1992. "On the Dissolved Oxygen Content in Seepage Water of the Open and the Closed System Percolation in a Stratified Soil Column." *Transaction of the Japanese Society of Irrigation, Drainage, and Reclamation Engineering* 159: 65-71.

[18] Iwate Agricultural Experimental Station. 1981. "Standard Investigation Method of Field Crops." Accessed April 1, 2016. http://www2.pref.iwate.jp/~hp2088/library/chousa/chousa_index.html.

[19] The Ministry of Agriculture, Forestry and Fisheries of Japan. 1979. "The Foundation of Environmental Paddy Field and Investigation of Paddy Field, Water Quality and Crop Analysis Method." In *National Conference of Paddy Field Preservation*, 113-5.

[20] Yamane, I. 1982. *Soil Science of Paddy Field*. Tokyo: Nobunkyo.

[21] Li, S., Sasaki, C., Kato, C., Matuyama, N., Annaka, T., Endo, A., et al. 2017. "Reducing Cadmium and Copper Uptake of Soybeans by Controlling Groundwater Level and Its Impacts on Growth and Yield." *International Journal of Environmental and Rural Engineering* 8: 77-84.

Journal of Environmental Science and Engineering A
Volume 7, Number 4, April 2018

David Publishing Company
616 Corporate Way, Suite 2-4876, Valley Cottage, NY 10989, USA
Tel: 1-323-984-7526, 323-410-1082; Fax: 1-323-984-7374, 323-908-0457
http://www.davidpublisher.com, www.davidpublisher.org
environmental@davidpublishing.org, environmental@davidpublishing.com

ISSN 2162-5298